Geosci. Model Dev. Discuss., 8, 9229–9279, 2015
www.geosci-model-dev-discuss.net/8/9229/2015/
doi:10.5194/gmdd-8-9229-2015

Geoscientific Model Development Discussions
Open Access
EGU

Oligomer formation in the troposphere: from experimental knowledge to 3-D modeling

V. Lemaire[1], I. Coll[1], F. Couvidat[2], C. Mouchel-Vallon[1], C. Seigneur[3], and G. Siour[1]

[1]LISA/IPSL, Laboratoire Interuniversitaire des Systè mes Atmosphériques, UMR CNRS 7583, Université Paris Est Créteil (UPEC) et Université Paris Diderot (UPD), 94010 Créteil, France
[2]INERIS, Institut National de l'Environnement Industriel et des Risques, Parc technologique ALATA, 60550, Verneuil en Halatte, France
[3]CEREA, Joint Laboratory Ecole des Ponts ParisTech/EDF R&D, Université Paris-Est (UPE), 77455 Marne la Vallée, France

Received: 26 August 2015 – Accepted: 13 October 2015 – Published: 28 October 2015

Correspondence to: I. Coll (isabelle.coll@lisa.u-pec.fr)

Published by Copernicus Publications on behalf of the European Geosciences Union.

Abstract

The organic fraction of atmospheric aerosols has proven to be a critical element of air quality and climate issues. However, its composition and the aging processes it undergoes remain insufficiently understood. This work builds on laboratory knowledge to simulate the formation of oligomers from biogenic secondary organic aerosol (BSOA) in the troposphere at the continental scale. We compare the results of two different modeling approaches, a 1st-order kinetic process and a pH-dependent parameterization, both implemented in the CHIMERE air quality model (AQM), to simulate the spatial and temporal distribution of oligomerized SOA over western Europe. Our results show that there is a strong dependence of the results on the selected modeling approach: while the irreversible kinetic process leads to the oligomerization of about 50 % of the total BSOA mass, the pH-dependent approach shows a broader range of impacts, with a strong dependency on environmental parameters (pH and nature of aerosol) and the possibility for the process to be reversible. In parallel, we investigated the sensitivity of each modeling approach to the representation of SOA precursor solubility (Henry's law constant values). Finally, the pros and cons of each approach for the representation of SOA aging are discussed and recommendations are provided to improve current representations of oligomer formation in AQMs.

1 Introduction

Due to their fast evolution in the troposphere and their continuous interaction with the ambient gas phase, atmospheric aerosols present a highly variable chemical composition in space and time (Q. Zhang et al., 2007). They comprise large quantities of inorganic species such as nitrates and sulfates, but they also contain an organic fraction (organic aerosol, OA), made of condensed semi-volatile organic species presenting a wide range of oxidation degrees (Jimenez et al., 2009). Part of this OA comes from the emission of particulate organic compounds into the atmosphere during combustion

GMDD
8, 9229–9279, 2015

processes: it is called Primary Organic Aerosol (POA). However, away from combustion emission sources, most of the OA arises from the oxidation of gas-phase organic species, making up the secondary organic aerosol (SOA), which may represent up to 70 % of OA on a mass basis (Kanakidou et al., 2005). The diversity in size and composition of atmospheric aerosols induces major differences in their physicochemical properties (Molnar et al., 2001; Kanakidou et al., 2005). These properties affect their impact on the radiative balance of the atmosphere (Stier et al., 2007; Paredes-Miranda et al., 2009) and their adverse health effects (Fuzzi et al., 2006). Thus, not only the total aerosol mass, but also their size distribution and their chemical content are of crucial importance for atmospheric issues. Although major scientific advances have been made during the last decade, the composition and the aging processes of the organic aerosol fraction remain insufficiently understood (e.g., Volkamer et al., 2006).

As a consequence, Air Quality Models (AQMs), despite significant progress, still have difficulties to quantitatively reproduce the observed particulate matter (PM) levels and gradients, and continue to underestimate the formation of SOA in the troposphere, from cities to remote areas (Shrivastava et al., 2011; Ervens et al., 2011; Petetin et al., 2014). In this regard, the chemistry of organics in the aqueous condensed phase remains poorly characterized. Thanks notably to atmospheric simulation chamber data, new processes have been integrated into AQMs so as to fill the gap between models and observations. These processes include for example the addition of new precursors (e.g., Y. Zhang et al., 2007), the treatment of SOA hygroscopicity (e.g., Pun, 2008) and aqueous chemistry SOA formation pathways (e.g., Carlton et al., 2008). In doing so, oligomerization was highlighted as one of the most important identified processes of SOA evolution. Laboratory studies indeed showed that oligomerization could be a quantitatively important evolution pathway for aqueous condensed species, and may greatly contribute to a better understanding of SOA aging (e.g., Kalberer et al., 2004; Jang et al., 2005; Trump and Donahue, 2014, and references therein). In particular, modeling studies have shown that the oligomerization of biogenic oxidized com-

GMDD
8, 9229–9279, 2015

pounds happens to be a significant source of secondary organic aerosols (Aksoyoglu et al., 2011).

Based on these experimental results, two distinct approaches aiming at representing oligomerization into AQMs have initially been developed. One approach, described by Carlton et al. (2010), proposes to represent the formation of oligomers observed in simulation chambers by using a first-order rate constant for all organic compounds. In parallel, Pun and Seigneur (2007) developed a pH-dependent oligomer formation, based on the experimental data of Jang et al. (2005), which applies only to the aldehyde species dissolved in the aerosol aqueous phase. More recently, Trump and Donahue (2014) also used an equilibrium approach to model oligomer formation within the volatility-basis set (VBS) formulation. Although these approaches rely on two very different concepts, they both aim to produce oligomers in the aerosol phase from the particle-phase reactions of condensed semi-volatile organic species, using empirical relationships. These parameterizations have been implemented in several AQMs such as CAMx (www.camx.com), CMAQ (http://www.cmaq-model.org) and Polyphemus (http://cerea.enpc.fr/polyphemus/index.html) in order to improve the simulated SOA concentration fields. Several modeling studies including these new parameterizations were conducted (Pun and Seigneur, 2007; Carlton et al., 2010; Aksoyoglu et al., 2011; Couvidat et al., 2012); it came out that oligomerization of biogenic oxidation products is mostly responsible for SOA formation and that the implementation of this process in AQMs reduces the discrepancy between the PM simulated mass and measurements in Europe and North America. However, although enhanced operational SOA modeling is needed, there still are no in situ measurements of oligomers that would increase our understanding of their formation and either allow the validation of these approaches or enable further refinement of the models. As an example, Pun and Seigneur (2007) indicated that their approach may overestimate the role of water in this process, as it is not currently known whether all liquid water present in aerosols is available to interact with organic compounds. Furthermore, as the two methods diverge both on the set of species submitted to oligomerization and on the nature of the

GMDD
8, 9229–9279, 2015

driving parameters (kinetic constant vs. equilibrium relationship), we also can expect the modeled distribution of simulated oligomers to differ between the two approaches.

To our knowledge, these approaches have not yet been compared in a same model. Such an initiative seems warranted, first to identify the range of uncertainties that these two parameterizations induce in the model outputs, but also to define how these parameterizations influence our understanding of SOA production in time and space. Thus, this work aims at investigating the representation of oligomerization that is provided by operational models. It consists in a model sensitivity study using, in turn, each oligomerization approach presented above to quantify the production of organic PM over Europe in the lower troposphere through continuous simulation. Moreover, it includes a study of the impact of the Henry's law constant computation for complex organic species, which is considered as a key parameter in representing the multiphase behavior of organic compounds in the atmosphere (Raventos et al., 2010). This study was conducted with the CHIMERE AQM (www.lmd.polytechnique.fr/chimere) at the continental scale over Europe during a summer period covering July and August 2006. The simulated SOA yields as well as the oligomer spatial and temporal distribution obtained in each model configuration are compared, so as to learn about the corresponding approaches.

This work is divided into three parts. First, the methodology and the model configurations are presented. Next the influence of the Henry' law constant on gas-particle partitioning, as well as the impact of each parameterization on the SOA budget are discussed. Finally, we discuss the assets and limitations of both oligomer modeling approaches and provide recommendations for future work.

2 Methodology and model set-up

2.1 Model set-up

This study uses the CHIMERE AQM, which is designed to produce daily forecasts of ozone, PM and other pollutants and to conduct pollution event analyses and re-

GMDD
8, 9229–9279, 2015

search studies in atmospheric chemistry (Menut et al., 2013). The model may be run from the regional to the continental scale, with horizontal resolutions ranging from 1 to 100 km. CHIMERE is used daily for operational air quality forecasts in 9 different regions of France and Europe. In this context, model performance is assessed every day via the comparison of the model output with atmospheric measurements, which also provides the basis for the ongoing improvement of CHIMERE. CHIMERE uses the MELCHIOR2 gas-phase chemical scheme (120 reactions among 44 gaseous species), which is adapted from the original EMEP mechanism and is a reduced version of the MELCHIOR1 mechanism, obtained by Carter's surrogate molecule method (Carter, 1990). The gas-phase chemical mechanism for SOA production has been described in detail by Pun et al. (2006) and Bessagnet et al. (2008).

In CHIMERE, a sectional aerosol module provides the evolution of the concentrations of 7 particulate groups of species: primary PM, nitrate, sulfate, ammonium, biogenic SOA, anthropogenic SOA, and water (Schmidt et al., 2001; Bessagnet et al., 2004, 2009). The size distribution of aerosol particles is represented using 8 size sections ranging from 10 to 40 µm. Physical processes taken into account are coagulation (Gelbard and Seinfeld, 1980), condensation via absorption (Nenes et al., 1998; Pun et al., 2006) and nucleation for sulfuric acid (Kulmala et al., 1988). The equilibrium concentrations of inorganic species are computed by the thermodynamic module ISORROPIA (version 1.7) presented in Nenes et al. (1988). The distribution of secondary organic species between the gas and particulate phases is calculated using Raoult's law with a temperature-dependent partitioning coefficient as described by Pankow (1994) for hydrophobic species and using Henry's law for hydrophilic species (Pun et al., 2006). In this version of the CHIMERE model, SOA formation is processed through the oxidation of 5 biogenic gaseous precursor species (isoprene, α-pinene, β-pinene, limonene, ocimene and humulene) and 4 anthropogenic precursor species (benzene, toluene, trimethylbenzene and a species accounting for C4-C10 alkanes). As for condensable species, both hydrophilic (condensation following Henry's law) and hydrophobic (condensation following Raoult's law) behaviors are considered, they are represented by:

GMDD
8, 9229–9279, 2015

- six hydrophilic surrogate species including an anthropogenic non-dissociative species (AnA0D), an anthropogenic once-dissociative species (AnA1D), an anthropogenic twice-dissociative species (AnA2D), a biogenic non-dissociative species (BiA0D), a biogenic once-dissociative species (BiA1D) and a biogenic twice-dissociative species (BiA2D). The pAnA*D and pBiA*D species stand for the part of the surrogate species that is present in the particulate phase

- three hydrophobic species comprising two anthropogenic species with low and moderate saturation vapor pressures (AnBIP and AnBmP) and a biogenic species with a moderate saturation vapor pressure (BiBmP)

- two water soluble surrogate species that account for the isoprene oxidation products (ISOPA1, ISOPA2). The oxidation of isoprene is adapted from the formulation prescribed by Kroll et al. (2006) and Y. Zhang et al. (2007).

Note that if – for any time step and grid cell – the modeled aerosol is not deliquescent, the gas-aerosol partition of the hydrophilic species will then be driven by their saturation vapor pressure. That is, their condensation will follow Raoult's law.

In the model, horizontal advection is calculated using the Van Leer second-order scheme and boundary layer turbulence is represented as a diffusion phenomenon, following Troen and Mahrt (1986). Vertical winds are diagnosed through a bottom-up mass balance scheme. Dry deposition is coded as in Wesely (1989) and photolytic rates are attenuated using liquid water or relative humidity. Finally, the numerical time solver uses the TWOSTEP method (Verwer, 1994).

The 2006 annual anthropogenic emissions from the EMEP (European Monitoring and Evaluation Programme) database (Vestreng et al., 2005) at a resolution of $0.5^{\circ} \times 0.5^{\circ}$ have been used (http://www.emep.int). They include CO, NH_3, NMVOC, NO_x, SO_x, and PM emissions for the 10 anthropogenic activity sectors of the SNAP nomenclature. The emission values are disaggregated into individual chemical species and at an hourly time step according to IER (Eber et al., 1994) recommendations, and are spatially distributed over our simulation domain using a kilometric land use

GMDD
8, 9229–9279, 2015

database (http://glcf.umiacs.umd.edu). Biogenic emissions have been computed with the MEGAN model (Guenther et al., 2006). Climatologic LMDZ (Hauglustaine et al., 2004) model output data were used for boundary conditions. Finally, the mesoscale model MM5 (Dudhia et al., 1993) was used to generate hourly meteorological fields for CHIMERE over a European domain covering our simulation domain, with a horizontal resolution of 54 km and using 32 levels in the vertical direction from the surface to 10 hPa.

A European domain extending from 6° W to 20° E in longitude and from 38 to 54° N in latitude (see Fig. 1) was defined for this study: its size allows tracking and studying large European city plumes and the domain includes our study area, which is western Europe. The horizontal resolution is 0.23° × 0.20°. For the vertical resolution, we used 8 levels of decreasing resolution from the ground level up to 500 hPa, the first model layer being 50 m thick. The simulation domain and its grid are illustrated in Fig. 1. The simulation period covers two months (July and August) in the summer of 2006. The simulation was run with a spin-up period (15 days) prior to the periods of interest in order to ensure that emissions and secondary pollutants are realistically distributed over the domain at the beginning of the evaluation period.

2.2 Oligomer parameterizations

This section describes the implementation of oligomer production in CHIMERE using the two existing parameterizations and their associated hypotheses.

2.2.1 Kinetic approach

The first approach (called hereafter KIN) is based on the hypothesis that oligomer formation may be represented through a kinetic process (Morris et al., 2006; Carlton et al., 2010). This hypothesis is supported by a series of smog chamber experiments conducted by Kalberer et al. (2004), where an important fraction of organic aerosol mass was shown to be composed of oligomers. The authors reported that, after 20 h

GMDD
8, 9229–9279, 2015

of processing, 50 % of the total organic aerosol mass was transformed into oligomers. From this result, Morris et al. (2006) proposed the use of a first-order rate constant $k_1 = 9.6 \times 10^{-6}\,s^{-1}$ to account for the oligomerization formation process, corresponding to a half-life of 20 h for organic species in the particulate phase. In this approach, biogenic and anthropogenic species are all potential oligomer precursors. However, due to low amounts of anthropogenic SVOC from the oxidation of classic precursors (toluene, xylene, trimethylbenzene...) over Europe, the production of anthropogenic oligomer could be negligible (Aksoyoglu et al., 2011).

To transcribe this approach in the model, we have allocated a first-order oligomer production kinetics to all the hydrophobic and hydrophilic surrogate species (AnA0-1-2D and BiA0-1-2D, AnBIP, AnBmP, BiBmP, ISOPA1 and ISOPA2) of the CHIMERE aerosol module. Preliminary simulations with CHIMERE confirmed the precedent findings, i.e. a very low budget of oligomers of anthropogenic origin (concentrations reach $10^{-3}\,ng\,m^{-3}$ at the maximum over the domain) compared with biogenic oligomers (which concentrations reach a few $\mu g\,m^{-3}$ for oligomers over many continental areas).

Thus, for simplification, only the 6 biogenic surrogate species (BiA0D, BiA1D, BiA2D, BiBmP, ISOPA1 and ISOPA2) were considered here (gas-phase chemical scheme for SOA formation is available in Table 6 of Menut et al., 2013). Furthermore, as will be discussed below, our study will focus on monoterpenes, a common species of both modeling approaches. To that end, a new species family called BiOLG, representing the total sum of oligomerized pBiA*D compounds, was introduced in CHIMERE. It accounts for oligomer formation from the oxidation of monoterpenes only and will be the basis for the intercomparison of the two approaches.

In this empirical parameterization, oligomerization is considered as an irreversible process. This approach has the advantage of simplicity, as it proposes a similar chemical reactivity for all organic oligomer precursors in the particulate phase (hydrophilic and hydrophobic species), one single chemical pathway for oligomer formation, and only one type of oligomer product. However, the drawback of this method is that it does not account for the details of the gas-phase SVOC speciation, for the variability

GMDD
8, 9229–9279, 2015

of the aerosol nature (deliquescent aerosol or not), nor for ambient parameters such as pH. Thus, it may lead to biases in the quantitative estimation of oligomer and OA production. Moreover, owing to the choice of a kinetic approach with a half life of 20 h, oligomer production is expected to be dominant away from source areas (except in the presence of severe anticyclonic conditions), enhancing the role of pollutant transport.

2.2.2 pH-dependant approach

The second approach (called here KPH) combines the laboratory works of Jang et al. (2005) – who showed that the polymerization of aldehydes may happen through a variety of acid-catalyzed reactions – and the observations of Gao et al. (2004) – who indicated that at least 10 % of the total organic aerosol mass is converted into oligomers due to the formation of organic acids in the aerosol. From these results, Pun and Seigneur (2007) developed an equation for the calculation of the gas-to-particle partitioning constant of semi-volatile aldehydes. It represents their increased partitioning toward the aqueous phase due to acidity:

$$K_{\mathrm{p,\,eff},\,i} = K_{\mathrm{p},\,i}\left[1 + K_{0,\,\mathrm{eff},\,i,\,\mathrm{ref}} \cdot \left(\frac{C_{\mathrm{H^+}}}{C_{\mathrm{H^+,\,ref}}}\right)^{1.91}\right] \quad (1)$$

where $K_{\mathrm{p,\,eff},\,i}$ is the effective partitioning coefficient of the ith compound between the gas phase and the aerosol aqueous phase; $K_{\mathrm{p},\,i}$ is its standard partitioning coefficient – calculated for non-acidic conditions – and $C_{\mathrm{H^+}}$ represent the aqueous concentration of hydronium ions. In this approach, $C_{\mathrm{H^+,\,ref}}$ is set to 10^{-6} mol L^{-1} and $K_{0,\,\mathrm{eff},\,i,\,\mathrm{ref}}$ stands for the value of 0.1 found by Gao et al. (2004) under the $C_{\mathrm{H^+,\,ref}}$ conditions. According to the results of Jang et al. (2005), aldehydes appear to be more reactive than ketones by two orders of magnitude. To simplify the parameterization, Pun and Seigneur (2007) considered as a first approximation that only aqueous aldehydes undergo oligomerization. In our model, it is equivalent to assuming that only BiA0D surrogates can lead to oligomer formation. Such a consideration derives from the fact that isoprene oxida-

GMDD
8, 9229–9279, 2015

tion products in CHIMERE are not associated with a given molecular structure. Thus, oligomerization processes could not be attributed to isoprene surrogates without more chemical details here, using the KPH approach. Our study then focuses on what can be learned from oligomerization modeling approaches on the basis of monoterpene surrogate reactivity.

Unlike the first approach, oligomerization is treated here as a reversible process. It is important to note that this approach only indirectly accounts for oligomer production. Indeed, to account for their aqueous reactivity, Eq. (1) alters the solubility of organic species, which in turn changes their particle-to-gas ratio and simulates their accumulation in the particulate phase. Thus, no model species is added to represent the aqueous oligomers. This is why it is necessary to perform two types of simulations to estimate the effect of the oligomerization process: a reference case – called hereafter REF – and a scenario case (KPH). The differences in the pBiA0D concentration fields between the two simulations represent aqueous oligomerization in the KPH approach:

$$[\text{Oligomers}] = [\text{pBiA0D}]_{\text{KPH}} - [\text{pBiA0D}]_{\text{REF}} \quad (2)$$

To implement this approach in the model and ensure the robustness of the modified partitioning constant value, it was necessary to adequately account for the acidity of the deliquescent particles. The particle pH is calculated in CHIMERE by an online coupling with the ISORROPIA model (http://nenes.eas.gatech.edu/ISORROPIA) that solves the transition between solid and aqueous phases through the estimation of the deliquescent relative humidity. However it is also possible to run ISORROPIA in a metastable configuration, which considers that aerosols remain in a liquid state, thus avoiding the transfer of dissolved BiA0D towards the gas phase under conditions of low relative humidity, thus favoring oligomer persistence and its transport in the atmosphere.

This alternative is taken into account for the evaluation of the KPH approach. ISORROPIA model also provides – for each cell and at every time step of the model calculation – particle water content and ion species equilibrium concentrations. At the end of the ISORROPIA computation, we constrained the particle pH to a range of values

GMDD
8, 9229–9279, 2015

between 2 and 6. The upper limit of 6 allows us to be consistent with the parameterization and to avoid partitioning constant values lower than that of the reference (see Eq. 1). The lower limit was set for numerical reasons, as the transfer of the concerned organic species to the aqueous phase becomes total under a pH of 2.

2.3 Module implementation

As mentioned in the previous section, isoprene oxidation products could not considered as oligomer precursors in the pH-dependent approach, due to the absence of structural information on these species in the gaseous chemical scheme. A refined chemical scheme for isoprene oxydation in CHIMERE is under development (Couvidat and Seigneur, 2011) and will be included later in the model. Pending this future model develoment, we focus here on a comparative evaluation of oligomerization of monoterpene oxidation products using the two parameterizations described above. Nevertheless, the absence of molecular structure allocation for ISOPA1 and ISOPA2 (model oxidation products of isoprene) is not a limiting factor for the kinetic approach. Thus, considerations about the relative importance of kinetic oligomer production from monoterpenes and isoprene will be presented in the result section.

One important issue in SOA production is the influence of the gas-particle partition of semi-volatile species on the final model results, whether under dry or wet conditions. However, since this work focuses on the reactivity of hydrophilic compounds, we specifically addressed the issue of Henry's constant values, K_H. By affecting the fraction of the semi-volatile species that partition into the aqueous phase, this constant directly impacts the quantitative production of the organic aerosol fraction. Furthermore, the reliability of K_H values is known to be low for complex compounds of atmospheric interest, especially for highly soluble species (Raventos et al., 2010). In order to observe the effect of refining these values in the different approaches, we ran the model with different sets of K_H values. To that end, the group contribution method of Suzuki et al. (1992) that is used by default in CHIMERE to produce K_H values at 298 K was replaced by a new group contribution approach called GROMHE, developed by Raventos

GMDD
8, 9229–9279, 2015

et al. (2010). This approach, which is based on the molecular structure of the molecule, was shown to be more reliable than the standard methods for complex organic compounds of atmospheric interest. By default, the molecular structure selected for BiA0D in CHIMERE is that of pinonaldehyde, a 10-carbon-atom molecule with an oxo group and an aldehyde group, while BiA1D and BiA2D are respectively based on norpinic acid (9-carbon-atom molecule with a carboxy group and an oxo group) and on pinic acid (9-carbon-atom molecule with two carboxy groups). Table 1 summarizes the default structure properties and molar masses, as well as the partitioning and saturation pressure characteristics used in CHIMERE for the 3 hydrophilic surrogates that lead to oligomer production from monoterpenes.

In order to evaluate the importance of considering a given molecular structure for each of these surrogate species, we computed different K_H values for them, corresponding to the different molecular structures they implicitly account for. The importance of investigating K_H values for our study is demonstrated in the next section (Sect. 3.1.1). Then, following the discussion of the results of the standard oligomerization approaches, we will discuss the results of additional oligomerization simulations conducted using a range of possible K_H values. These sensitivity tests are presented in detail in Sect. 3.2.

3 Results

3.1 Model approaches for oligomer formation

3.1.1 Precursor partitioning in the reference case

In order to examine the gas-particle partition of the model surrogates, we report in Fig. 2 the average concentration fields of the hydrophilic and hydrophobic surrogates simulated by CHIMERE in the reference case for the period 20 July–3 August 2006. This figure indicates that BiA1D is the highest hydrophilic contributor to the organic

GMDD
8, 9229–9279, 2015

aerosol mass concentration, while BiA0D remains quasi-exclusively in the gas phase. However, among the monoterpene surrogates, the hydrophobic species BiBmP is the largest contributor to the organic aerosol mass concentration. On average, hydrophilic and hydrophobic species account for 25 and 75 % of this organic aerosol mass concentration, respectively.

As the impact of the K_H partitioning constant value is likely to be important for the formation of oligomers, we focused on gaseous hydrophilic species and on the processes governing their transfer toward the particulate phase. To that end, we analyzed two different situations. In the first one, the aerosol is treated as a deliquescent aerosol where the distribution of the hydrophilic species between the gas and the condensed phases is driven by Henry's law. In the second one, we consider a dry aerosol where the partition of hydrophilic species is driven by Raoult's law.

For the deliquescent aerosol situation, we calculated the partitioning coefficient as described by Mouchel-Vallon et al. (2013), where the fraction of the surrogate species in the aqueous phase is obtained as follows:

$$\xi^i = \frac{C_a^i}{C_a^i + C_g^i} = \left(1 + \frac{1}{H^i RTL}\right)^{-1} \quad (3)$$

In this equation, C_a^i and C_g^i represent (in $\mu g\,m^{-3}$) the concentration of species i in the particulate and gas phases respectively; H_i is the Henry's law constant (in $M\,atm^{-1}$); R is the ideal gas law constant; T is the temperature, and L is the liquid water content (LWC) of the aerosol (in cm^3 liquid water cm^{-3} air). We set the liquid water content value within the 10^{-11}–10^{-12} range of values proposed by Engelhart et al. (2011) for a deliquescent aerosol.

For a dry aerosol we used an equation similar to Eq. (3), which has been shown to apply equally to the organic compounds that condense into an organic phase (e.g., Donahue et al., 2009; Valorso et al., 2011). There, M_w stands for the mean organic aerosol molar mass (set to $250\,g\,mol^{-1}$ based on Robinson et al. (2007), C_{OA} repre-

GMDD
8, 9229–9279, 2015

sents the total organic aerosol mass concentration ($\mu g\,m^{-3}$) and P_{vap} is the saturation vapor pressure (atm) and considering an ideal mixture.

$$\xi^i = \frac{C_a^i}{C_a^i + C_g^i} = \left(1 + \frac{M_w P_{vap}}{C_{OA} RT}\, 10^6\right)^{-1} \quad (4)$$

Figure 3 illustrates the gas-particle partition of the three semi-volatile compounds considered in our work for the two distinct situations. The fraction of the compound present in the particulate phase (represented by ξ_i values) is plotted as a function of K_H for a deliquescent aerosol under typical atmospheric liquid water content situations (upper graph), and as a function of P_{vap} in the case of a dry organic aerosol with C_{OA} ranging from low ($0.1\,\mu g\,m^{-3}$) to high ($10\,\mu g\,m^{-3}$) atmospheric concentrations (lower graph). This figure shows how the magnitude of the condensation process increases with the K_H value (Fig. 3a) and decreases with the saturation vapor pressure (Fig. 3b). To analyze these results, each graph can be split into 3 parts.

For deliquescent aerosols:

- When the Henry's law constant value is lower than $10^7\,M\,atm^{-1}$ (part I) or greater than $10^{13}\,M\,atm^{-1}$ (part III), then whatever the value of LWC, the equilibrium is either totally in favor of the gas phase (part I, insoluble compounds) or in favor of the particulate phase (part III, soluble compounds), respectively.
- For intermediate K_H values (part II), the mass of the semi-volatile species is shared between the two phases. In this area, partitioning towards the aqueous phase is an increasing function of LWC values.

Similarly, for dry aerosols:

- The partition is completely in favor of the aerosol phase (low volatility compounds – part 1) or towards the gas phase (volatile compounds – part 3) whatever the C_{OA} for saturation vapor pressures that are lower than 10^{-13} atm or greater than 10^{-6} atm, respectively.

GMDD
8, 9229–9279, 2015

– For intermediate values (part 2, shaded area), partitioning towards the condensed phase increases with increasing C_{OA}.

The main conclusions that can be drawn from these graphs are the following. First, over this set of atmospheric situations, and whatever the nature of the aerosol – BiA0D never contributes significantly to OA formation. Indeed, ξ_{BiA0D} values reach a maximum of 0.3 % in the most favorable combination (dry aerosol, $C_{OA} = 10\,\mu g\ m^{-3}$). Second, ξ_{BiA1D} and ξ_{BiA2D} values respectively range from 1.7 to 14.4 % and from 1.5 to 12.9 % for a deliquescent aerosol, and span the 3.30–77.4 % and the 4.9–83.9 % ranges in the presence of a dry aerosol. Thus, BiA1D and BiA2D are likely to sweep a wide range of partitioning states in the presence of a dry aerosol, while their K_H value are too low to account for a substantial transfer to the aqueous aerosol phase in the presence of a deliquescent aerosol. One should note, however, that in the dry aerosol model (Eq. 4), the activity coefficients are assumed to be unity; in other words, one does not account for interactions among organic species. Since hydrophobic and hydrophilic species have significantly different molecular structures, one could anticipate that including the activity coefficients in the model would reduce the absorption of the hydrophilic species in the hydrophobic organic phase or even lead to the formation of a separate organic phase (Couvidat and Sartelet, 2015). Therefore, the values given for the partition of hydrophilic aerosol should be seen as upper limits. Considering those 2 elements, K_H appears to be an influential parameter for BiA*D species, its modulation – with regard to the effective solubility of the surrogates – being likely to strongly enhance the oligomer production efficiency when the aerosol is deliquescent and when the residual gas fraction of the surrogate is not negligible. A species such as BiA0D, which currently remains mostly gaseous in the standard version of the model, may thus be particularly sensitive to the reference value of its Henry's law partitioning constant.

It is thus important to determine how uncertainties in the K_H value influence the results and efficiency of the two oligomer production approaches. For this purpose, we conducted sensitivity tests to the refinement of the most uncertain K_H values, taking into account the structure of the model species and of its components.

GMDD
8, 9229–9279, 2015

3.1.2 Oligomer production from the oxidation of monoterpenes

CHIMERE simulations were launched in the reference, KIN, and KPH configurations (both modes) for the two periods of interest defined above. The quantitative differences in the concentrations of the simulated biogenic oligomers, as well as their spatial and temporal features, were investigated. As mentioned previously, we focused on the comparison between the BiOLG (KIN approach) and the $pBiA0D_{KPH-REFERENCE}$ (KPH approaches) concentration fields.

Figure 4 presents the oligomer daily concentration maxima simulated by CHIMERE from the oxidation of monoterpenes for both parameterizations and for one representative day of the simulated period. It highlights large differences in the oligomer concentration fields produced in each approach, both in terms of intensity and spatial distribution. Indeed we can see that, using the KIN approach, the highest oligomer concentrations reach about 0.80 $\mu g\,m^{-3}$ over southeastern Europe (Fig. 4a) while in both KPH configurations the peak values are highly localized (not necessary in the same areas according to the mode used) and may exceed 1 $\mu g\,m^{-3}$ (Fig. 4b and c), with local peaks around 1.50 $\mu g\,m^{-3}$ (not visible on the color scale). The same discrepancies between the KIN and the KPH model configurations are observed for every day of the summer period, with daily concentration maxima spanning the 0.30–1 $\mu g\,m^{-3}$ and the 0.80–2.50 $\mu g\,m^{-3}$ ranges, respectively. In terms of hourly peaks, we can learn from the KPH results that there are areas of high gaseous precursor concentrations where BiA0D solubility is (at least transiently) strongly enhanced by local reductions in pH. According to Fig. 3 the decline in pH has to be greater than 3 or 4 units with regard to the reference value of 6, so as to increase the BiA0D partitioning constant by several orders of magnitude and allow the massive transfer of the species to the particulate phase. Such conditions appear to be met off the eastern Italian and over well-delimited forested continental areas of northern Spain notably. From the elevated peak values, it seems likely that the formation of oligomers proceeds by rapid changes in the BiA0D partitioning. In return, the inhomogeneity of oligomer concentration fields

GMDD
8, 9229–9279, 2015

suggests a recurring evaporation of the particulate aerosol component in the deliquescent mode and/or the instability of low pH values. As for the KIN approach, we can see that the time required for the kinetic process as well as the irreversible nature of the coded process allow the presence of large regional oligomer plumes with smooth concentration gradients, as well as the presence of significant amounts of this species over the entire domain.

When averaging our results over the whole summer period, we observe no significant change in the location of high oligomer concentrations, though concentration values are logically lower than hourly peaks, and concentration fields show smoother gradients. However what is interesting is that the quantitative trends differ from those observed previously (Fig. 5). Indeed, the KIN parameterization produces the highest average oligomer concentrations that range from 0.1 to 0.4 $\mu g\,m^{-3}$ over most of the simulation domain. This approach forms well-mixed secondary plumes similar to those of other long-lived atmospheric oxidants such as ozone, with maxima over Central Europe and Mediterranean areas. On the contrary, KPH oligomers only slightly exceed 0.1 $\mu g\,m^{-3}$ in both deliquescent and metastable modes, except over small regions of the Adriatic Sea and over northern Spain areas where they only reach up to 0.3 $\mu g\ m^{-3}$ in the deliquescent mode. It is noticeable that, due to the persistence of an aqueous phase, the metastable mode produces higher oligomer concentrations over the entire domain. However, the difference remains moderate in terms of absolute mass concentration. This feature confirms the lack of oligomer mass accumulation in the KPH approach that was observed in the spatial analysis of hourly maps. Beyond this, it indicates that favorable conditions for oligomers production are not often met along time. The conditions of the process reversibility have to be more precisely identified and understood, for both modes of the KPH approach.

3.1.3 Driving parameters of both approaches

We explored these differences in order to identify the parameters driving production, transport and decomposition of oligomers over continental areas for both approaches.

GMDD
8, 9229–9279, 2015

First, the parameters describing the aerosol properties together with the BiA0D partition were plotted over the domain and analyzed for a given time step of the simulation. Then we investigated the temporal evolution of the BiA0D partition and oligomer formation at one grid point of the domain in the 3 CHIMERE configurations.

Figure 6 presents the nature (humid or dry) and the pH of the aerosol simulated over Europe for 24 July 2006 at 05:00 UTC, in relation with BiA0D concentration fields. The similarity of the aerosol type (dry or humid, Fig. 6a) determined by ISORROPIA and of the oligomer concentration fields (Fig. 6d) indicates that the existence of a deliquescent aerosol is not ensured in all grid cells and proves to be a discriminatory parameter for oligomer production in the simulations. Figure 6 also emphasizes the role of pH in this process. In northern Spain, significant oligomer formation is observed in the presence of both a wet aerosol and a very acidic aqueous phase (pH around 2.5), although this is not a region where the concentrations of BiA0D are high. On the contrary, over Great-Britain, where there is no significant oligomer formation, CHIMERE predicts the presence of a deliquescent aerosol, low gaseous BiA0D concentrations and a pH value around 4. These results place the pH threshold for a significant oligomer production from BiA0D at a value comprised between 3 and 4. Our previous calculations indicate that the fraction of BiA0D in the aerosol phase remains lower than 1 % for a pH of 4, but reaches up to 6–39 % for a pH of 3, considering a LWC in the 10^{-11} to 10^{-12} range ($cm^3\,water\,cm^{-3}$). This exponential relationship supports the local formation of high oligomers concentration peaks in Fig. 6d, with regards to the conditions shown in Fig. 6a and b. Clearly, although the presence of the precursor is the first requirement for oligomer production, it is not a determining parameter of the structure of oligomer concentration fields. As the modeled pH strongly impacts the rate and the intensity of oligomer formation, its robustness was questioned. Although no direct measurements of the pH of the aerosol have been realized yet, our calculations are consistent with previous experimental studies reporting strongly acidic fine particles (Ludwig and Klemm, 1990; Herrmann, 2003; Keene et al., 2004). Our results are also consistent with the work of Xue et al. (2011), which is based on chemical composition and meteorological

GMDD
8, 9229–9279, 2015

data collected at a suburban site in Hong Kong and which estimated the aerosol pH to range between −1.87 and 3.12.

In order to address the temporal variation of the aerosol properties related with oligomer formation, concentration time series for BiA0D (reference simulation – blue line) and for oligomers (KIN approach – red line, KPH approach – green line for the deliquescent mode, black line for the metastable mode) have been plotted in Fig. 7 for a given grid cell in northern Spain for the period from 20 to 24 July.

In the KIN approach, BiOLG progressively accumulates in the air mass and shows a smoothed concentration curve along time. Furthermore, oligomer concentrations are not strongly correlated with the presence of gaseous precursors due to the time required for the kinetic formation process. In the KPH approach, oligomer concentrations are highly variable, showing intense peaks that alternate with periods of near-zero content in the particle phase. It is noted that the black curve (KPH, metastable mode) present high values on 22 and 23 July that are not observed for the results of the deliquescent mode. These events are not either correlated with a specific origin of the air mass (analysis not shown here) or with a given BiA0D concentration threshold, but both take place during shaded periods and can therefore be attributed to the limiting effect of a dry aerosol in the deliquescent mode. However, from the co-variability of pBiA0D concentrations in shaded and non-shaded areas, it appears that the existence of a deliquescent aerosol is not the only driving parameter of this formation/evaporation cycle. Indeed, sharp decreases in the particulate fraction of BiA0D are simultaneously observed whatever the aerosol physic state (see 21–22 and 24 July for instance), which implies that pH variability also plays a decisive role during a large part of the day. During these periods, the pH was indeed comprised between 4 and 6, thus being the principal limitation for BiA0D storage in the particulate phase. Thereby, whatever the selected mode (deliquescent or metastable), there is no continental transport of oligomers due to evaporation processes. It results in the simulation of short duration peaks, accounting for local production from emissions.

GMDD
8, 9229–9279, 2015

Finally, Fig. 7 reveals the recurrent loss of particulate BiA0D in northern Spain during the period of study, mostly during daytime periods. It shows an average duration of 2 to 6 h for the oligomer peak events, which is quite short in view of the time required for pollutant mixing and transport in the troposphere. Therefore, these local phenomena cannot affect PM mixing ratios over large areas and for extended time periods. As the transfer of BiA0D to the gas phase from the aerosol is frequent and total in the KPH approach, its consistency has to be considered. This process appears to be highly dependent both on the pH variability – which has been poorly measured up to now – and on the K_H correcting factor necessary to alter the partition of BiA0D between the 2 phases. That is, the choice of the reference K_H value may be of primary importance. Such findings question the relevance of simulating a low-constrained reversibility for the formation of oligomers in 3-D models.

From these results, three key points can be inferred. First, the structure of oligomer concentration fields is driven both by the kinetic constant rate and by average pBiA*D concentrations in the KIN approach, while it mainly depends on the physical and chemical areosol properties in the KPH approach. In that latter approach, the formation of large quantities of oligomers appears to be conditional on the presence of a deliquescent aerosol and of strong acidity, sufficient initial particulate material, and possibly high radical levels for the oxidation of biogenic VOCs. However, most of the differences between this equilibrium approach and the kinetic one may be reduced by considering a greater stability (better constrained reversibility) in the pH-dependent oligomerization process. The relevance of taking this into consideration in 3D models will be discussed in the last part of this article. Second, the total mass of simulated oligomers, as well as their participation in the organic fraction of the aerosol, is clearly specific to the adopted approach. This is quantitatively described in Sect. 3.1.4. Finally, we have shown that the default solubility to BiA0D is a determining element of the model results in the KPH approach. As it affects the default quantities of BiA0D (and other oligomer precursors) in the aerosol, it may also play a major role in the results of the KIN approach. As the

GMDD
8, 9229–9279, 2015

allocation of this parameter is quite uncertain, the sensitivity of the model results to K_H will be investigated in Sect. 3.2.

3.1.4 Oligomer to organic aerosol ratio in summer

In a second step, we estimated the contribution of the modeled oligomers to the biogenic secondary organic aerosol (BSOA) budget. For this analysis, we first considered the ratio of oligomers arising from monoterpenes only to the so-called $BSOA_{terp}$ (fraction of SOA induced by both hydrophilic and hydrophobic species from monoterpenes, Fig. 8) and then, using the KIN approach only, all biogenic (isoprene included) oligomers (Fig. 9) and total BSOA.

When considering monoterpenes as the only oligomer precursors, the implementation of a kinetic approach (Fig. 8, left and central upper graphs) results in a significant increase (+1–2 $\mu g\,m^{-3}$) of the average OA mass concentration inside the plume. Although the general structure of the plumes is not changed, the kinetic production of oligomers leads to the presence of significant $BSOA_{terp}$ values over an area that is much broader than in the reference case. On the opposite, the KPH approach in deliquescent mode (Fig. 8, right upper graph) does not modify the average mass concentration and spatial distribution of $BSOA_{terp}$. The same conclusion can be drawn from the metastable version of KPH (not shown here). In terms of ratios, the OA fraction that remains under the form of oligomers (Fig. 8, lower graphs representing pOLG to $BSOA_{terp}$ ratio) represents 20 to 50 % of the organic aerosol mass originating in monoterpenes over all the continental areas in the KIN approach. It is due to the stabilization of a very large proportion of biogenic organic species in the condensed phase under the form of oligomers. However, extreme values of this ratio are simulated over marine areas (see the purple color, meaning that approximately 80 % of $BSOA_{terp}$ is under the form of oligomers). This phenomenon can be explained by a combination of two factors. First, irreversible and continuous oligomer formation is the only possible chemical evolution pathway for condensed biogenic species in this version of the model. Second, in our model, marine areas are very little influenced by fresh organic

GMDD
8, 9229–9279, 2015

emissions, which tend to favor the omnipresence of an aged OA over the sea. This is probably wrong, as high contributions of primary organic matter to the marine aerosol were observed. However, they are not taken into account in our simulations (Ovadnevaite et al., 2011). Furthermore, such a high degree of OA conversion to oligomers has never been reported in the literature. Although it is limited on that point, it may be partly unrealistic to simulate a single fate for all biogenic organics present in the particulate phase. Despite this statement, the absolute OA concentration simulated over the sea remains low ($< 0.2\,\mu g\,m^{-3}$), thereby limiting the impact of this potential bias in the model. In regards to KPH simulations, the model indicates (as expected) a very low average contribution of oligomers to the mass of $BSOA_{terp}$ over continental areas, except in the north of Spain – where the contribution of oligomers represents 10 to 20 % of the SOA mass concentration – and over marine areas where it sometimes exceeds 40 %. Over continental areas, the oligomer fraction is shown to be insignificant because of the frequent reversal of the formation process due to wide pH variations (see above).

Isoprene oxidation products are a major contributor (around 50 % in our simulations) to the total SOA mass. Therefore, when their potential for oligomerization is considered in KIN, they significantly contribute to this aged organic fraction. Indeed, as can be seen in Fig. 9, when isoprene surrogates are included in the OA aging process, the average BSOA mass fraction increases by 2 to $4\,\mu g\,m^{-3}$ over the whole eastern and southern areas of our domain. In these areas, its total concentrations reach 3 to $6\,\mu g\,m^{-3}$. The largest increases are obtained over Italy, as well as over the Mediterranean and Adriatic Seas, where the recirculation of continental air masses possibly favors air mass aging under low dispersion conditions.

These results highlight the importance of closer identifying the oxidation products of the main atmospheric BVOCs, as well as their structure and reactivity. In particular, questions still arise about the way the evolution of condensed isoprene derivatives should be represented. Indeed, the assumption of Carlton et al. (2010), which states that the formation of oligomers is driven by a same first-order rate constant whatever the oxidation products, is questionable. First, because this parameterization derives

GMDD
8, 9229–9279, 2015

from the evolution of cyclic compounds in chamber experiments, which is the case of α- and β-pinene, the 2 most common monoterpenes, but not of isoprene and its derivatives. The oxidation of isoprene by hydroxyl radicals leads to the formation of methyl vinyl ketone and methacrolein (Pandis et al., 1991; Paulot et al., 2009), which in turn produce tetrols and methylglyceric acid (Claeys et al., 2004; Surratt et al., 2006; Kleindienst et al., 2009) that are aliphatic compounds. Although oligomer formation from the oxidation of isoprene has been shown to occur in smog chambers (e.g., Sato et al., 2011; Nguyen et al., 2011a, b; Liu et al., 2012a; Tan et al., 2012; Lin et al., 2014), the oligomer formation process is likely to differ significantly from that from aromatics as measured by Kalberer et al. (2004) Second, because this kinetic constant only stands for an average reactivity as Kalberer et al. (2004), during their experiments, could only observe the fact that 50 % of the total organic mass was conversed to oligomer-like species. Such results cannot establish whether all aromatic compounds had undergone oligomerization following the same pathway or if its evolution was only attributable to a specific set of compounds. Applying this parameterization to a large set of biogenic species may cause an incorrect assessment of the contribution of oligomers to the total SOA budget.

3.2 Sensitivity to the K_H value

From the model results presented in Figs. 4 to 7, we found that the amplitude of oligomer formation was potentially strongly dependent on the reference K_H value of BiA0D, whatever approach is taken. Yet, the solubility of Bia0D has to be considered as an uncertain parameter. First because Bia0D accounts for 11 monoterpenes oxidation products, which partition differently and may be poorly approximated via a unique K_H value. Second, because it is recognized that, regardless of the group contribution approach used, uncertainties in the estimation of K_H grow when solubility exceeds 10^4 M atm^{-1}, due to a lack of experimental measurements (Raventos et al., 2010). This is an important issue as all the 11 species represented by pinonaldehyde all have a solubility greater than that of pinonaldehyde itself ($K_H = 4.97 \times 10^4$ M atm^{-1}).

GMDD
8, 9229–9279, 2015

This is notably the case of hydroxypinonaldehyde ($K_H = 3.26 \times 10^7$ M atm^{-1}), ketolimonoaldehyde ($K_H = 1.7 \times 10^8$ M atm^{-1}) or 2-hydroxy-3-iso-propyl-6-oxo-heptanal ($K_H = 2.5 \times 10^6$ M atm^{-1}). Consequently, it appears warranted to consider the possibility for the BiA0D Henry's law constant to vary by several orders of magnitude. Thus, in order to evaluate the robustness of each approach to this input parameter, sensitivity tests to the solubility of the BiA0D species were conducted with CHIMERE.

3.2.1 Influence on the surrogate partitioning properties

In view of surrogate properties presented in Fig. 3a, our sensitivity study focused on the transition area, that is the 4×10^8–4×10^9 M atm^{-1} range of K_H, which allows accounting for the solubility of all the potential oxidation products mentioned before, while providing estimates of the impact of correcting the global BiA0D K_H value. In this range, we considered 3 specific K_H values for BiA0D (4.97×10^4, 4×10^8 and 4×10^9 M atm^{-1}). Before conducting the sensitivity tests in CHIMERE, we evaluated the influence of K_H on the partitioning coefficient of BiA0D, using the same graphs as in Sect. 2, over the whole range of possible pH values and with a liquid water content of 10^{-11} cm^3 water cm^{-3}. The results are presented in Fig. 10. The reference value ($K_H = 4.97 \times 10^4$ M atm^{-1}, black curve of Fig. 10) corresponds to the left part of Fig. 3a, that is a quite null value of the partitioning coefficient. Here, we can see that only an acidic aqueous phase (pH < 4) allows the quantitative formation of oligomers. When increasing K_H to a value in the 4×10^8 to 4×10^9 M atm^{-1} range, we enter the second area of Fig. 3a, where the particulate fraction of BiA0D becomes significant for a LWC of 10^{-11} cm^3 water cm^{-3}). There, a significant formation of SOA takes place from neutral conditions with 10 % to 52 % of BiA0D being in the condensed phase, depending on the K_H value. For a pH of 5, particulate fraction reaches 48 and 90 % in favor of the aerosol phase, for $K_H = 4 \times 10^8$ and 4×10^9 M atm^{-1} respectively. However, in this transition area, the partition of the surrogate species remains strongly influenced by the liquid water content. Such results underline the threshold condensation phenomenon for this range of K_H values. Also,

GMDD
8, 9229–9279, 2015

such a sensitivity of BiA0D solubility to the K_H value may have important consequences for the results of the KPH approach (whatever the mode considered). Indeed, considering the highest K_H value instead of the standard one, at pH = 6, in the reference simulations, causes the reference particulate fraction of BiA0D to increase from 0 to 52 % (with LWC = 10^{-11} cm^3 water cm^{-3}). The impact of implementing a pH-dependent approach will thus be lower and the resulting speciation of the OA material will show a much lesser proportion of oligomers.

3.2.2 Impact on the simulated oligomer concentration fields

The sensitivity tests were launched with CHIMERE in the reference, KIN and KPH configurations (in both deliquescent and metastable modes) using each time a different K_H value, as mentioned in the previous section. The average simulated oligomer concentrations fields are shown in Fig. 11 for the KIN (left), KPH deliquescent (center) and KPH metastable (right) approaches.

In the KIN approach, we observe that an increase in the value of the Henry's law constant value (from top to bottom, left column) induces an increase in average simulated oligomer concentrations, due to the low initial solubility of the BiA0D species, which was identified as a limiting parameter for the kinetic production of oligomer in the condensed phase. However, this dependency exhibits a threshold phenomenon, as the increase of K_H by almost 4 orders of magnitude (from 4.97×10^4 to 4×10^8 M atm^{-1}) induces approximately the same response (0.1 to 0.2 µg m^{-3} of increase over Italy and the Adriatic Sea) as a further increase by one order of magnitude (4×10^8 to 4×10^9 M atm^{-1}).

The interpretation of the model results is more complex in the KPH configuration. As stated above, the KPH parameterization affects the partition between the gas and particulate phases, and oligomer concentrations are accounted for by an increase in the quantities of the condensed surrogate BiA0D. For the deliquescent mode, when K_H is set to 4×10^8 M atm^{-1} (Fig. 11e), oligomer concentrations increase over continental areas on average by 0.1 to 0.2 µg m^{-3} compared with the simulation using the

GMDD
8, 9229–9279, 2015

standard K_H value (Fig. 11b). Indeed, as the solubility of Bia0D grows, the decrease in pH required to form particulate material is reduced. Thus, even for pH values around 4–5, the partitioning of BiA0D towards the aerosol is increased. When shifting again the K_H value by one order of magnitude ($K_H = 4 \times 10^9\,\mathrm{M\,atm^{-1}}$; Fig. 11h), we observe a decrease in the oligomer concentrations compared with Fig. 11e. This result illustrates the fact that the modification of the BiA0D partition creates less oligomer when K_H exceeds a given threshold. Indeed, the fraction of BiA0D in the condensed phase is by default substantial and there is thus no significant effect of adding an oligomer production parameterization. However, the total pBiA0D mass (already dissolved + produced from the modification of K_H) increases with K_H, from the top (Fig. 11b) to the bottom (Fig. 11h) scenario. As regards the metastable mode, the absolute increase in the oligomer concentration due to acidity is significantly higher than in the deliquescent mode (see the concentration scale that is 4 times larger compared with the KIN and KPH deliquescent maps) as the dependence upon relative humidity was removed. However, the same conclusions as for the deliquescent mode can be drawn.

Finally, whatever the initial choice of BiA0D solubility, the location and the spatial extent of oligomer formation remain different in the 3 configurations of CHIMERE. While the kinetic production of oligomer species leads to a diffuse plume reaching many remote areas of Europe, the highest concentrations of oligomers are definitely observed close to biogenic source areas in the KPH approaches. It is worthy to note that the KPH metastable configuration – associated with high K_H values for BiA0D – also allows the formation of large continental plumes, which is not observed in the deliquescent mode. This last configuration makes little sense, as the KPH approach is based on the possibility for OA formation to depend on the specificities of the aerosol aqueous phase which is no longer the case in Fig. 11e and h. However, as the plumes differ from those of the KIN approach, it brings our attention on the importance of oligomer formation rate from gaseous precursors, and on the number/types of precursors.

GMDD
8, 9229–9279, 2015

4 Discussions and conclusions

In view of oligomer concentrations simulated by CHIMERE using two different approaches, several points need to be discussed.

First, the oligomer concentrations in both approaches are highly influenced by the initial value of K_H. Yet 3-D models use one single value of this parameter to account for the behavior of a complex mixture of SOA precursors and this parameter is unable to restitute entirely the variability of the gas/particle partitioning of all these compounds in time and space. It is interesting to see that allocating a high default value to K_H allows an immediate transfer of SVOCs into the condensed phase and thus increase significantly the organic aerosol concentration in continental plumes. As rapid oligomer formation was observed in laboratory experiments, imposing a minimum value for K_H could be a substitute to oligomer formation processes (which require the addition of chemical reactions) and reduce significantly the size of chemical scheme in AQMs. However, this choice may affect the spatio-temporal distribution of organic aerosol as can be deduced from the large differences between the KIN and KPH oligomer plumes. It thus appears necessary to refine the Henry's law constant values of the SVOCs of atmospheric interest.

Second, improvements and developments could be considered for each approach. As for the KIN parameterization, it would be important to propose distinct values for the kinetic constants of the various oligomer precursors, in particular as Kalberer et al. (2006) have shown disparities in the temporal evolution of the aerosol molar mass considering the oxidation of trimethylbenzene, α-pinene and isoprene. Regarding KPH, one single oligomerization pathway is represented for all environmental conditions. This is one main limitations of the approach. Furthermore, its dependence on the nature and state (deliquescent or metastable) of the aerosol, as well as its pH – all determined by the ISORROPIA model – is probably overestimated.

But, more significantly, the two approaches differ on the irreversible (KIN) or reversible (KPH) property of the oligomerization process which, from our findings, is

GMDD
8, 9229–9279, 2015

one key point of this process. According to a recent study of Wang et al. (2010), the heterogeneous reactions forming oligomers on nanoparticules may be at least partially irreversible, as their persistence in the particulate phase upon water evaporation should be effective due to their their low volatility and their high molecular weight (Wang et al., 2010; Ervens et al., 2011; Liu et al., 2012b). This assumption is supported by the recent works of Hall and Johnston (2012a) who investigated the thermal stability of a SOA matrix including 50 % of oligomeric species formed by the ozonolysis of α-pinene: the authors concluded that, at ambient temperatures, oligomeric species should be nonvolatile by structure. These observations cannot be reproduced with the KPH-deliquescent approach as the production of OA is canceled right after each phase of water evaporation or pH increase. In the light of the recent experimental results mentionned above, a potential improvement of the KPH approach could be the addition of reactive uptake in aerosol, as for the KIN parameterization. Indeed, it is now recognized that organic compounds may undergo chemical reactions in the particle phase by both non-oxidative and oxidative reactions that lead to the formation of semi-volatile compounds and even non-volatile compounds in the case of high molecular weight species (Kroll and Seinfeld, 2008; Kroll et al., 2009). Furthermore, through laboratory experiments conducted on ozonolysis of α–pinene, oligomer formation would be driven by reactive uptake rather than by the partition of monomers between both phases (Hall and Johnson, 2012b). Nevertheless, this reactive uptake being observed within seconds (Heaton et al., 2007; Hall and Johnson, 2012b) it appears more realistic to represent the oligomerization process in two steps: a first fast step modifying directly the partitioning of monomers to represent the rapid formation of oligomers before the stabilization of the OA formed through a reactive uptake. Currently, the KIN approach does not allow this initial step.

In view of all these elements, a KPH-like approach using a metastable mode and considering a reactive uptake with partial reversibility could be a suitable parameterization to represent the formation of oligomers from monoterpenes. However the determination of the aerosol mode is not an obvious choice (Fountoukis et al., 2009). Moya

GMDD
8, 9229–9279, 2015

et al. (2002) have shown that considering a metastable mode for PM_1 (where organic matter is mainly present) leads, under low relative humidity conditions (< 60 %), to significant errors in the concentrations of the inorganic species which indirectly determine the aerosol pH and thus oligomers formation. The authors conclude that it is essential to consider a deliquescent mode for low relative humidity.

Concerning isoprene, we have mentioned the fact that it is recognized as an important precursor of SOA through its first generation products, methacrolein (MACR) and methyl vinyl ketone (MVK) (Pandis et al., 1991; Carlton et al., 2009). During recent experimental studies these compounds have been detected as important oligomer precursors in the condensed phase (El Haddad et al., 2009; Liu et al., 2012b; Renard et al., 2013). Renard et al. (2015), for instance, investigated the formation of oligomers through the photooxidation of MVK into a photoreactor. This study revealed that considering only a first-order rate constant to represent the formation of oligomers is not appropriate. Indeed, they highlighted that the oxidation of MVK by OH (in the condensed phase of a deliquescent aerosol) is governed by a kinetic competition between functionalization and oligomerization, depending on the precursor initial concentration. Furthermore, even if the oxidation mechanisms in the condensed phase are assumed to be the same as in the gas phase, the branching ratio in favor of highly oxidized monomers seems to be more important than in the gas phase (Kroll and Seinfeld, 2008). Furthermore, based on the laboratory experiments of Renard et al. (2015), Ervens et al. (2015) developed a chemical mechanism for the oligomerization of MVK and MACR in a deliquescent aerosol. Using a multiphase box model, they underlined the potential key role of MVK to oxygen concentration ratio in the oligomerization rate, under atmospherically relevant conditions. Thus, the oligomerization process of isoprene derivatives constitutes a complex atmospheric multiphase process where a kinetic approach is probably relevant to represent the initial formation of oligomers, but a second-order rate constant would be more suitable than the current first-order rate constant to represent the oxidation of first-generation isoprene products by $OH_{(aq)}$. However, further experimental work about MVK and MACR aqueous reactivity is needed to consolidate the

GMDD
8, 9229–9279, 2015

experimental findings before implementing such chemical schemes in AQMs. As an example, Ervens et al., (2015) proposed a k_{oligo} of 2.50×10^{-12} molec cm^{-3} s^{-1} for the single oxidation reaction of MVK (or MACR) by hydroxyl radical to form oligomers, but they recommend being cautious with this value due to the fact that the kinetics could be different when considering different atmospheric conditions (LWC, $OH_{(aq)}$, MACR, MVK concentrations...).

Acknowledgements. This work was supported by the French national program PRIMEQUAL in the frame of the OLDAIR project.

References

Aksoyoglu, S., Keller, J., Barmpadimos, I., Oderbolz, D., Lanz, V. A., Prévôt, A. S. H., and Baltensperger, U.: Aerosol modelling in Europe with a focus on Switzerland during summer and winter episodes, Atmos. Chem. Phys., 11, 7355–7373, doi:10.5194/acp-11-7355-2011, 2011.

Bessagnet, B., Hodzic, A., Vautard, R., Beekmann, M., Cheinet, S., Honore, C., Liousse, C., and Rouil, L.: Aerosol modeling with CHIMERE – preliminary evaluation at the continental scale, Atmos. Environ., 38, 2803–2817, doi:10.1016/j.atmosenv.2004.02.034, 2004.

Bessagnet, B., Menut, L., Curci, G., Hodzic, A., Guillaume, B., Liousse, C., Moukhtar, S., Pun, B., Seigneur, C., and Schulz, M.: Regional modeling of carbonaceous aerosols over Europe-focus on secondary organic aerosols, J. Atmos. Chem., 61, 175–202, doi:10.1007/s10874-009-9129-2, 2008.

Bessagnet, B., Menut, L., Curci, G., Hodzic, A., Guillaume, B., Liousse, C., Moukhtar, S., Pun, B., Seigneur, C., and Schulz, M.: Regional modeling of carbonaceous aerosols over Europe-focus on secondary organic aerosols, J. Atmos. Chem., 61, 175–202, 2009.

Carlton, A. G., Turpin, B. J., Altieri, K. E., Seitzinger, S. P., Mathur, R., Roselle, S. J., and Weber, R. J.: CMAQ model performance enhanced when in-cloud secondary organic aerosol is included: comparisons of organic carbon predictions with measurements, Environ. Sci. Technol., 42, 8798–8802, doi:10.1021/es801192n, 2008.

GMDD

8, 9229–9279, 2015

Carlton, A. G., Wiedinmyer, C., and Kroll, J. H.: A review of Secondary Organic Aerosol (SOA) formation from isoprene, Atmos. Chem. Phys., 9, 4987–5005, doi:10.5194/acp-9-4987-2009, 2009.

Carlton, A. G., Bhave, P. V., Napelenok, S. L., Edney, E. D., Sarwar, G., Pinder, R. W., Pouliot, G. A., and Houyoux, M.: Model representation of secondary organic aerosol in CMAQv4.7, Environ. Sci. Technol., 44, 8553–8560, doi:10.1021/es100636q, 2010.

Carter, W. P. L.: A detailed mechanism for the gas-phase atmospheric reactions of organic-compounds, Atmos. Environ. A-Gen., 24, 481–518, doi:10.1016/0960-1686(90)90005-8, 1990.

Couvidat, F. and Sartelet, K.: The Secondary Organic Aerosol Processor (SOAP v1.0) model: a unified model with different ranges of complexity based on the molecular surrogate approach, Geosci. Model Dev., 8, 1111–1138, doi:10.5194/gmd-8-1111-2015, 2015.

Couvidat, F. and Seigneur, C.: Modeling secondary organic aerosol formation from isoprene oxidation under dry and humid conditions, Atmos. Chem. Phys., 11, 893–909, doi:10.5194/acp-11-893-2011, 2011.

Couvidat, F., Debry, E., Sartelet, K., and Seigneur, C.: A hydrophilic/hydrophobic organic (H^2O) aerosol model: developmentn evaluation and sensitivity analysis, J. Geophys. Res., 117, D10304, doi:10.1029/2011JD017214, 2012.

Claeys, M., Graham, B., Vas, G., Wang, W., Vermeylen, R., Pashynska, V., Cafmeyer, J., Guyon, P., Andreae, M. O., Artaxo, P., and Maenhaut, W.: Formation of secondary organic aerosol through photooxidation of isoprene, Science, 303, 1173–1176, doi:10.1126/science.1092805, 2004.

Donahue, N. M., Robinson, A. L., and Pandis, S. N.: Atmospheric organic particulate matter: from smoke to secondary organic aerosol, Atmos. Environ., 43, 94–106, 2009.

Dudhia, J.: A nonhydrostatic version of the Penn State-NCAR Mesoscale model: validation tests and simulation of an Atlantic cyclone and cold front, Mon. Weather Rev., 121, 1493–1513, doi:10.1175/1520-0493(1993)121<1493:ANVOTP>2.0.CO;2, 1993.

Eber, A., Friedrich, R., and Rodhe, H.: Tropospheric modelling and emission estimation: Generation of european emission data for episodes (genemis) project, eurotrac annual report 1993, part 5, 1994.

El Haddad, I., Yao Liu, Nieto-Gligorovski, L., Michaud, V., Temime-Roussel, B., Quivet, E., Marchand, N., Sellegri, K., and Monod, A.: In-cloud processes of methacrolein under simulated

GMDD
8, 9229–9279, 2015

conditions – Part 2: Formation of secondary organic aerosol, Atmos. Chem. Phys., 9, 5107–5117, doi:10.5194/acp-9-5107-2009, 2009.
Ervens, B., Turpin, B. J., and Weber, R. J.: Secondary organic aerosol formation in cloud droplets and aqueous particles (aqSOA): a review of laboratory, field and model studies, Atmos. Chem. Phys., 11, 11069–11102, doi:10.5194/acp-11-11069-2011, 2011.
Ervens, B., Renard, P., Tlili, S., Ravier, S., Clément, J.-L., and Monod, A.: Aqueous-phase oligomerization of methyl vinyl ketone through photooxidation – Part 2: Development of the chemical mechanism and atmospheric implications, Atmos. Chem. Phys., 15, 9109–9127, doi:10.5194/acp-15-9109-2015, 2015.
Fountoukis, C., Nenes, A., Sullivan, A., Weber, R., Van Reken, T., Fischer, M., Matías, E., Moya, M., Farmer, D., and Cohen, R. C.: Thermodynamic characterization of Mexico City aerosol during MILAGRO 2006, Atmos. Chem. Phys., 9, 2141–2156, doi:10.5194/acp-9-2141-2009, 2009.
Fuzzi, S., Andreae, M. O., Huebert, B. J., Kulmala, M., Bond, T. C., Boy, M., Doherty, S. J., Guenther, A., Kanakidou, M., Kawamura, K., Kerminen, V.-M., Lohmann, U., Russell, L. M., and Pöschl, U.: Critical assessment of the current state of scientific knowledge, terminology, and research needs concerning the role of organic aerosols in the atmosphere, climate, and global change, Atmos. Chem. Phys., 6, 2017–2038, doi:10.5194/acp-6-2017-2006, 2006.
Gao, S., Ng, N. L., Keywood, M., Varutbangkul, V., Bahreini, R., Nenes, A., He, J. W., Yoo, K. Y., Beauchamp, J. L., Hodyss, R. P., Flagan, R. C., and Seinfeld, J. H.: Particle phase acidity and oligomer formation in secondary organic aerosol, Environ. Sci. Technol., 38, 6582–6589, doi:10.1021/es049125k, 2004.
Gelbard, F. and Seinfeld, J. H.: Simulation of multicomponent aerosol dynamics, J. Colloid Interf. Sci., 78, 485–501, doi:10.1016/0021-9797(80)90587-1, 1980.
Guenther, A., Karl, T., Harley, P., Wiedinmyer, C., Palmer, P. I., and Geron, C.: Estimates of global terrestrial isoprene emissions using MEGAN (Model of Emissions of Gases and Aerosols from Nature), Atmos. Chem. Phys., 6, 3181–3210, doi:10.5194/acp-6-3181-2006, 2006.
Hall, W. A. and Johnston, M. V.: Oligomer content of α-pinene secondary organic aerosol, Aerosol Sci. Tech., 45, 37–45, 2011.
Hall, W. A. and Johnston, M. V.: The thermal-stability of oligomers in alpha-pinene secondary organic aerosol, Aerosol Sci. Tech., 46, 983–989, 2012a.

GMDD
8, 9229–9279, 2015

Hall, W. A. and Johnston, M.: Oligomer formation pathways in secondary organic aerosol from MS and MS/MS measurements with high mass accuracy and resolving power, J. Am. Soc. Mass Spectr., 23, 1097–1108, 2012b.

Hauglustaine, D., Hourdin, F., Jourdain, L., Filiberti, M.-A., Walters, S., Lamarque, J.-F., and Holland, E.: Interactive chemistry in the Laboratoire de Météorologie Dynamique general circulation model: description and background tropospheric chemistry evaluation, J. Geophys. Res.-Atmos., 109, D04314, doi:10.1029/2003JD003957, 2004.

Herrmann, H.: Kinetics of aqueous phase reactions relevant for atmospheric chemistry, Chem. Rev., 103, 4691–4716, 2003.

Jang, M. S., Czoschke, N. M., and Northcross, A. L.: Semiempirical model for organic aerosol growth by acid-catalyzed heterogeneous reactions of organic carbonyls, Environ. Sci. Technol., 39, 164–174, doi:10.1021/es048977h, 2005.

Jimenez, J. L., Canagaratna, M. R., Donahue, N. M., Prevot, A. S. H., Zhang, Q., Kroll, J. H., DeCarlo, P. F., Allan, J. D., Coe, H., Ng, N. L., Aiken, A. C., Docherty, K. S., Ulbrich, I. M., Grieshop, A. P., Robinson, A. L., Duplissy, J., Smith, J. D., Wilson, K. R., Lanz, V. A., Hueglin, C., Sun, Y. L., Tian, J., Laaksonen, A., Raatikainen, T., Rautiainen, J., Vaattovaara, P., Ehn, M., Kulmala, M., Tomlinson, J. M., Collins, D. R., Cubison, M. J., Dunlea, E. J., Huffman, J. A., Onasch, T. B., Alfarra, M. R., Williams, P. I., Bower, K., Kondo, Y., Schneider, J., Drewnick, F., Borrmann, S., Weimer, S., Demerjian, K., Salcedo, D., Cottrell, L., Griffin, R., Takami, A., Miyoshi, T., Hatakeyama, S., Shimono, A., Sun, J. Y., Zhang, Y. M., Dzepina, K., Kimmel, J. R., Sueper, D., Jayne, J. T., Herndon, S. C., Trimborn, A. M., Williams, L. R., Wood, E. C., Middlebrook, A. M., Kolb, C. E., Baltensperger, U., and Worsnop, D. R.: Evolution of organic aerosols in the atmosphere, Science, 326, 1525–1529, doi:10.1126/science.1180353, 2009.

Kalberer, M., Paulsen, D., Sax, M., Steinbacher, M., Dommen, J., Prevot, A. S. H., Fisseha, R., Weingartner, E., Frankevich, V., Zenobi, R., and Baltensperger, U.: Identification of polymers as major components of atmospheric organic aerosols, Science, 303, 1659–1662, doi:10.1126/science.1092185, 2004.

Kalberer, M., Sax, M., and Samburova, V.: Molecular size evolution of oligomers in organic aerosols collected in urban atmospheres and generated in a smog chamber, Environ. Sci. Technol., 40, 5917–5922, 2006.

Kanakidou, M., Seinfeld, J. H., Pandis, S. N., Barnes, I., Dentener, F. J., Facchini, M. C., Van Dingenen, R., Ervens, B., Nenes, A., Nielsen, C. J., Swietlicki, E., Putaud, J. P., Balkan-

GMDD
8, 9229–9279, 2015

ski, Y., Fuzzi, S., Horth, J., Moortgat, G. K., Winterhalter, R., Myhre, C. E. L., Tsigaridis, K., Vignati, E., Stephanou, E. G., and Wilson, J.: Organic aerosol and global climate modelling: a review, Atmos. Chem. Phys., 5, 1053–1123, doi:10.5194/acp-5-1053-2005, 2005.

Keene, W. C., Pszenny, A. A. P., Maben, J. R., Stevenson, E., and Wall, A. C. D.: Closure evaluation of size-resolved aerosol pH in the New England coastal atmosphere during summer, J. Geophys. Res.-Atmos., 109, D23307, doi:10.1029/2004JD004801, 2004.

Kroll, J. H. and Seinfeld, J. H.: Chemistry of secondary organic aerosol: formation and evolution of low-volatility organics in the atmosphere, Atmos. Environ., 42, 3593–3624, doi:10.1016/j.atmosenv.2008.01.003, 2008.

Kroll, J. H., Ng, N. L., Murphy, S. M., Flagan, R. C., and Seinfeld, J. H.: Secondary organic aerosol formation from isoprene photooxidation, Environ. Sci. Technol., 40, 1869–1877, 2006.

Kroll, J. H., Smith, J. D., Che, D. L., Kessler, S. H., Worsnop, D. R., and Wilson, K. R.: Measurement of fragmentation and functionalization pathways in the heterogeneous oxidation of oxidized organic aerosol, Phys. Chem. Chem. Phys., 11, 8005–8014, 2009.

Kulmala, M., Laaksonen, A., and Pirjola, L.: Parameterizations for sulfuric acid/water nucleation rates, J. Geophys. Res.-Atmos., 103, 8301–8307, doi:10.1029/97jd03718, 1998.

Lin, Y.-H., Budisulistiorini, S. H., Chu, K., Siejack, R. A., Zhang, H., Riva, M., Zhang, Z., Gold, A., Kautzman, K. E., and Surratt, J. D.: Light-absorbing oligomer formation in secondary organic aerosol from reactive uptake of isoprene epoxydiols, Environ. Sci. Technol., 48, 12012–12021, 2014.

Liu, Y., Monod, A., Tritscher, T., Praplan, A. P., DeCarlo, P. F., Temime-Roussel, B., Quivet, E., Marchand, N., Dommen, J., and Baltensperger, U.: Aqueous phase processing of secondary organic aerosol from isoprene photooxidation, Atmos. Chem. Phys., 12, 5879–5895, doi:10.5194/acp-12-5879-2012, 2012.

Liu, Y., Siekmann, F., Renard, P., El Zein, A., Salque, G., El Haddad, I., Temime-Roussel, B., Voisin, D., Thissen, R., and Monod, A.: Oligomer and SOA formation through aqueous phase photooxidation of methacrolein and methyl vinyl ketone, Atmos. Environ., 49, 123–129, 2012b.

Ludwig, J. and Klemm, O.: Acidity of size-fractionated aerosol-particles, Water Air Soil Pollut., 49, 35–50, doi:10.1007/bf00279508, 1990.

Menut, L., Bessagnet, B., Khvorostyanov, D., Beekmann, M., Blond, N., Colette, A., Coll, I., Curci, G., Foret, G., Hodzic, A., Mailler, S., Meleux, F., Monge, J.-L., Pison, I., Siour, G., Tur-

GMDD
8, 9229–9279, 2015

quety, S., Valari, M., Vautard, R., and Vivanco, M. G.: CHIMERE 2013: a model for regional atmospheric composition modelling, Geosci. Model Dev., 6, 981–1028, doi:10.5194/gmd-6-981-2013, 2013.

Molnar, A. and Meszaros, E.: On the relation between the size and chemical composition of aerosol particles and their optical properties, Atmos. Environ., 35, 5053–5058, doi:10.1016/s1352-2310(01)00314-4, 2001.

Moya, M., Pandis, S. N., and Jacobson, M. Z.: Is the size distribution of urban aerosols determined by thermodynamic equilibrium?: an application to Southern California, Atmos. Environ., 36, 2349–2365, 2002.

Mouchel-Vallon, C., Bräuer, P., Camredon, M., Valorso, R., Madronich, S., Herrmann, H., and Aumont, B.: Explicit modeling of volatile organic compounds partitioning in the atmospheric aqueous phase, Atmos. Chem. Phys., 13, 1023–1037, doi:10.5194/acp-13-1023-2013, 2013.

Nenes, A., Pandis, S. N., and Pilinis, C.: ISORROPIA: a new thermodynamic equilibrium model for multiphase multicomponent inorganic aerosols, Aquat. Geochem., 4, 123–152, doi:10.1023/a:1009604003981, 1998.

Nguyen, T. B., Roach, P. J., Laskin, J., Laskin, A., and Nizkorodov, S. A.: Effect of humidity on the composition of isoprene photooxidation secondary organic aerosol, Atmos. Chem. Phys., 11, 6931–6944, doi:10.5194/acp-11-6931-2011, 2011a.

Nguyen, T. B., Laskin, J., Laskin, A., and Nizkorodov, S. A.: Nitrogen-containing organic compounds and oligomers in secondary organic aerosol formed by photooxidation of isoprene, Environ. Sci. Technol., 45, 6908–6918, 2011b.

Ovadnevaite, J., O'Dowd, C., Dall'Osto, M., and Ceburnis, D.: Detecting high contributions of primary organic matter to marine aerosol: a case study, Geophys. Res. Lett., 38, L02807, doi:10.1029/2010GL046083, 2011.

Pandis, S. N., Paulson, S. E., Seinfeld, J. H., and Flagan, R. C.: Aerosol formation in the photooxidation of isoprene and β-pinene, Atmos. Environ. A-Gen., 25, 997–1008, 1991.

Pankow, J. F.: An absorption-model of gas-particle partitioning of organic-compounds in the atmosphere, Atmos. Environ., 28, 185–188, doi:10.1016/1352-2310(94)90093-0, 1994.

Paredes-Miranda, G., Arnott, W. P., Jimenez, J. L., Aiken, A. C., Gaffney, J. S., and Marley, N. A.: Primary and secondary contributions to aerosol light scattering and absorption in Mexico City during the MILAGRO 2006 campaign, Atmos. Chem. Phys., 9, 3721–3730, doi:10.5194/acp-9-3721-2009, 2009.

GMDD
8, 9229–9279, 2015

Petetin, H., Beekmann, M., Sciare, J., Bressi, M., Rosso, A., Sanchez, O., and Ghersi, V.: A novel model evaluation approach focusing on local and advected contributions to urban $PM_{2.5}$ levels – application to Paris, France, Geosci. Model Dev., 7, 1483–1505, doi:10.5194/gmd-7-1483-2014, 2014.

Paulot, F., Crounse, J. D., Kjaergaard, H. G., Kroll, J. H., Seinfeld, J. H., and Wennberg, P. O.: Isoprene photooxidation: new insights into the production of acids and organic nitrates, Atmos. Chem. Phys., 9, 1479–1501, doi:10.5194/acp-9-1479-2009, 2009.

Pun, B. K.: Development and initial application of the sesquiversion of MADRID, J. Geophys. Res.-Atmos., 113, 10, doi:10.1029/2008jd009888, 2008.

Pun, B. K. and Seigneur, C.: Investigative modeling of new pathways for secondary organic aerosol formation, Atmos. Chem. Phys., 7, 2199–2216, doi:10.5194/acp-7-2199-2007, 2007.

Pun, B. K., Seigneur, C., and Lohman, K.: Modeling secondary organic aerosol formation via multiphase partitioning with molecular data, Environ. Sci. Technol., 40, 4722–4731, doi:10.1021/es0522736, 2006.

Raventos-Duran, T., Camredon, M., Valorso, R., Mouchel-Vallon, C., and Aumont, B.: Structure-activity relationships to estimate the effective Henry's law constants of organics of atmospheric interest, Atmos. Chem. Phys., 10, 7643–7654, doi:10.5194/acp-10-7643-2010, 2010.

Renard, P., Siekmann, F., Gandolfo, A., Socorro, J., Salque, G., Ravier, S., Quivet, E., Clément, J.-L., Traikia, M., Delort, A.-M., Voisin, D., Vuitton, V., Thissen, R., and Monod, A.: Radical mechanisms of methyl vinyl ketone oligomerization through aqueous phase OH-oxidation: on the paradoxical role of dissolved molecular oxygen, Atmos. Chem. Phys., 13, 6473–6491, doi:10.5194/acp-13-6473-2013, 2013.

Renard, P., Siekmann, F., Salque, G., Demelas, C., Coulomb, B., Vassalo, L., Ravier, S., Temime-Roussel, B., Voisin, D., and Monod, A.: Aqueous-phase oligomerization of methyl vinyl ketone through photooxidation – Part 1: Aging processes of oligomers, Atmos. Chem. Phys., 15, 21–35, doi:10.5194/acp-15-21-2015, 2015.

Robinson, A. L., Donahue, N. M., Shrivastava, M. K., Weitkamp, E. A., Sage, A. M., Grieshop, A. P., Lane, T. E., Pierce, J. R., and Pandis, S. N.: Rethinking organic aerosols: semivolatile emissions and photochemical aging, Science, 315, 1259–1262, doi:10.1126/science.1133061, 2007.

Sato, K., Nakao, S., Clark, C. H., Qi, L., and Cocker III, D. R.: Secondary organic aerosol formation from the photooxidation of isoprene, 1,3-butadiene, and 2,3-dimethyl-1,3-butadiene

GMDD
8, 9229–9279, 2015

under high NO_x conditions, Atmos. Chem. Phys., 11, 7301–7317, doi:10.5194/acp-11-7301-2011, 2011.
Schmidt, H., Derognat, C., Vautard, R., and Beekmann, M.: A comparison of simulated and observed ozone mixing ratios for the summer of 1998 in Western Europe, Atmos. Environ., 35, 6277–6297, doi:10.1016/s1352-2310(01)00451-4, 2001.
Shrivastava, M., Fast, J., Easter, R., Gustafson Jr., W. I., Zaveri, R. A., Jimenez, J. L., Saide, P., and Hodzic, A.: Modeling organic aerosols in a megacity: comparison of simple and complex representations of the volatility basis set approach, Atmos. Chem. Phys., 11, 6639–6662, doi:10.5194/acp-11-6639-2011, 2011.
Stier, P., Seinfeld, J. H., Kinne, S., and Boucher, O.: Aerosol absorption and radiative forcing, Atmos. Chem. Phys., 7, 5237–5261, doi:10.5194/acp-7-5237-2007, 2007.
Suzuki, T., Ohtaguchi, K., and Koide, K.: Application of principal components-analysis to calculate Henry constant from molecular-structure, Comput. Chem., 16, 41–52, doi:10.1016/0097-8485(92)85007-l, 1992.
Tan, Y., Lim, Y. B., Altieri, K. E., Seitzinger, S. P., and Turpin, B. J.: Mechanisms leading to oligomers and SOA through aqueous photooxidation: insights from OH radical oxidation of acetic acid and methylglyoxal, Atmos. Chem. Phys., 12, 801–813, doi:10.5194/acp-12-801-2012, 2012.
Troen, I. and Mahrt, L.: A simple-model of the atmospheric boundary-layer – sensitivity to surface evaporation, Bound.-Lay. Meteorol., 37, 129–148, doi:10.1007/bf00122760, 1986.
Trump, E. R. and Donahue, N. M.: Oligomer formation within secondary organic aerosols: equilibrium and dynamic considerations, Atmos. Chem. Phys., 14, 3691–3701, doi:10.5194/acp-14-3691-2014, 2014.
Valorso, R., Aumont, B., Camredon, M., Raventos-Duran, T., Mouchel-Vallon, C., Ng, N. L., Seinfeld, J. H., Lee-Taylor, J., and Madronich, S.: Explicit modelling of SOA formation from α-pinene photooxidation: sensitivity to vapour pressure estimation, Atmos. Chem. Phys., 11, 6895–6910, doi:10.5194/acp-11-6895-2011, 2011.
Verwer, J. G.: Gauss–Seidel iteration for Stiff ODEs from chemical kinetics, SIAM J. Sci. Comput., 5, 1243–1250, 1994.
Vestreng, V., Breivik, K., Adams, M., Wagner, A., Goodwin, J., Rozovsk aya, O., and Pacyna, J. M.: Inventory Review 2005 – Emission Data reported to CLRTAP and under the NEC Directive – Initial review for HMs and POPs, EMEP/MSC-W, available at: http:

GMDD
8, 9229–9279, 2015

//acm.eionet.europa.eu/reports/EMEP_MSC-W_Techn_Rep_1_2005 (last access: 27 October 2015), 2005.
Volkamer, R., Jimenez, J. L., San Martini, F., Dzepina, K., Zhang, Q., Salcedo, D., Molina, L. T., Worsnop, D. R., and Molina, M. J.: Secondary organic aerosol formation from anthropogenic air pollution: rapid and higher than expected, Geophys. Res. Lett., 33, 4, doi:10.1029/2006gl026899, 2006.
Wang, L., Khalizov, A. F., Zheng, J., Xu, W., Ma, Y., Lal, V., and Zhang, R. Y.: Atmospheric nanoparticles formed from heterogeneous reactions of organics, Nat. Geosci., 3, 238–242, doi:10.1038/ngeo778, 2010.
Xue, J., Lau, A. K. H., and Yu, J. Z.: A study of acidity on PM(2.5) in Hong Kong using online ionic chemical composition measurements, Atmos. Environ., 45, 7081–7088, 2011.
Zhang, Q., Jimenez, J. L., Canagaratna, M. R., Allan, J. D., Coe, H., Ulbrich, I., Alfarra, M. R., Takami, A., Middlebrook, A. M., Sun, Y. L., Dzepina, K., Dunlea, E., Docherty, K., DeCarlo, P. F., Salcedo, D., Onasch, T., Jayne, J. T., Miyoshi, T., Shimono, A., Hatakeyama, S., Takegawa, N., Kondo, Y., Schneider, J., Drewnick, F., Borrmann, S., Weimer, S., Demerjian, K., Williams, P., Bower, K., Bahreini, R., Cottrell, L., Griffin, R. J., Rautiainen, J., Sun, J. Y., Zhang, Y. M., and Worsnop, D. R.: Ubiquity and dominance of oxygenated species in organic aerosols in anthropogenically-influenced Northern Hemisphere midlatitudes, Geophys. Res. Lett., 34, 6, doi:10.1029/2007gl029979, 2007.
Zhang, Y., Huang, J.-P., Henze, D. K., and Seinfeld, J. H. C. D.: Role of isoprene in secondary organic aerosol formation on a regional scale, J. Geophys. Res.-Atmos., 112, D20207, doi:10.1029/2007JD008675, 2007.

GMDD
8, 9229–9279, 2015

Table 1. Properties of the biogenic hydrophilic and hydrophobic surrogate SOA species used in the simulations conducted with the CHIMERE model.

Surrogate species	Molecular Structure	Molar Mass ($g\,mol^{-1}$)	Henry's law constant[1] ($M\,atm^{-1}$ at 298 K)	Saturation vapor pressure[2] (atm)	Considered in KIN[3]	Considered in KPH[3]
BiA0D	Pinonaldehyde	168	4.97×10^{4}	3.55×10^{-7}	Yes	Yes
BiA1D	Norpinic acid	170	6.85×10^{8}	2.86×10^{-10}	Yes	No
BiA2D	Pinic acid	186	6.03×10^{8}	1.88×10^{-10}	Yes	No
BiBmP	C15 oxo aldehyde	236	10^{-2}	3.97×10^{-9}	Yes	No

[1] The Henry's law constants are calculated with the group contribution approach, GROMHE.
[2] Pun et al. (2006).
[3] Surrogate undergoing oligomerization.

GMDD
8, 9229–9279, 2015

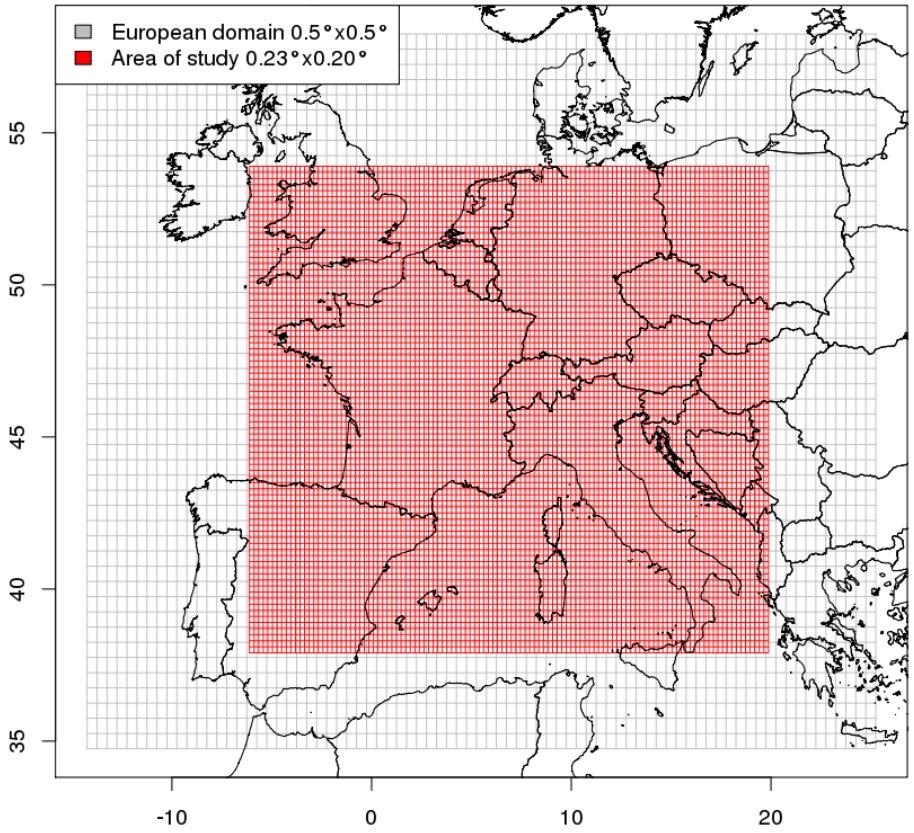

Figure 1. In red, gridded domain used for the air quality simulations, having a horizontal resolution of 0.23° × 0.20°. In black, large-scale domain used to provide boundary conditions (horizontal resolution of 0.5° × 0.5°).

GMDD
8, 9229–9279, 2015

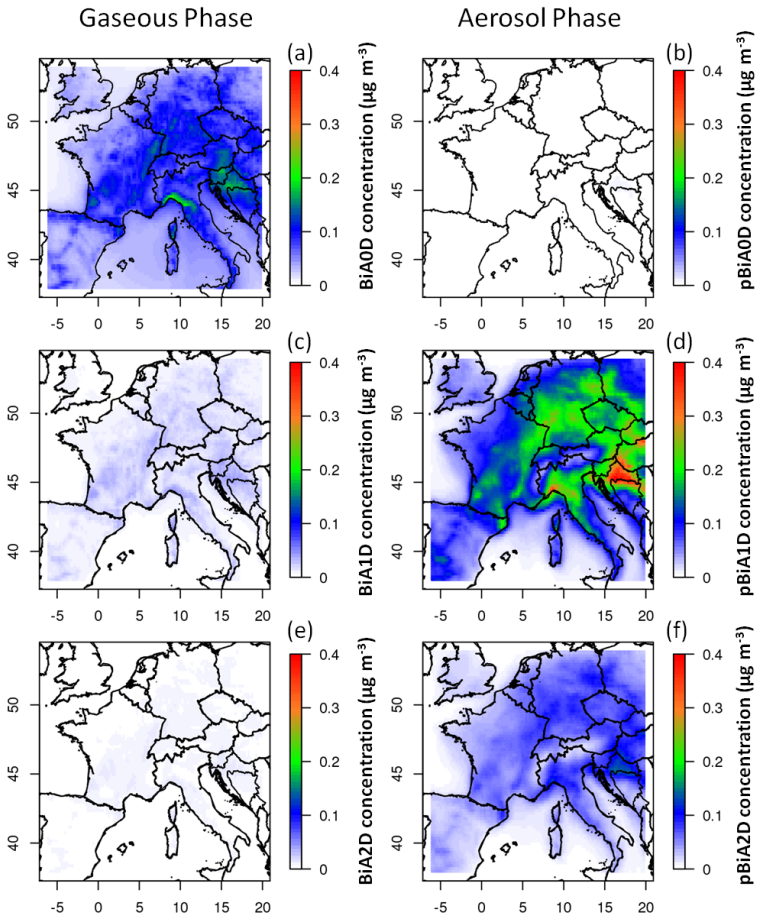

Figure 2. Mass concentration fields of BiA0D (**a** and **b**), BiA1D (**c** and **d**), BiA2D (**e** and **f**) and BiBmP (**g** and **h**) in the gas (left) and particulate (right) phases, modeled by CHIMERE and averaged over 20 July–3 August 2006.

GMDD
8, 9229–9279, 2015

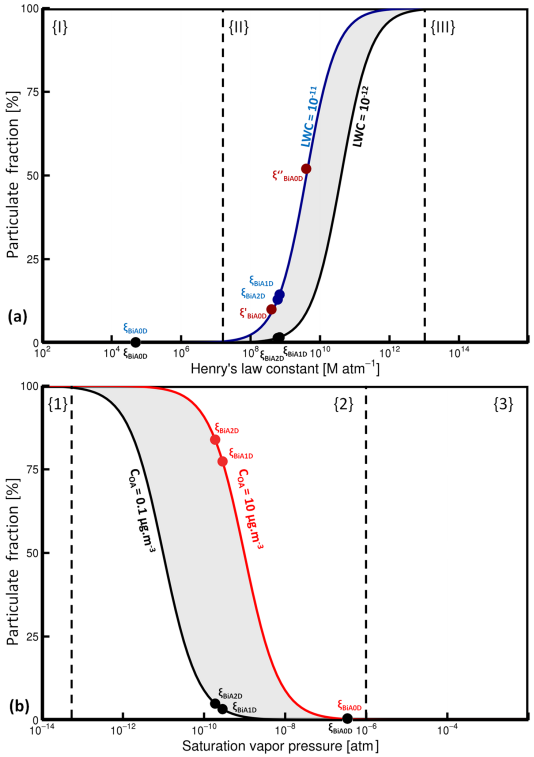

Figure 3. Particulate fraction as a function of Henry's law constant (upper figure) and as a function of saturation vapor pressure (lower figure). The partition of each surrogate is represented by the colored dots for different conditions of organic aerosol mass concentration. Shaded areas represent the range of typical atmospheric condition.

GMDD
8, 9229–9279, 2015

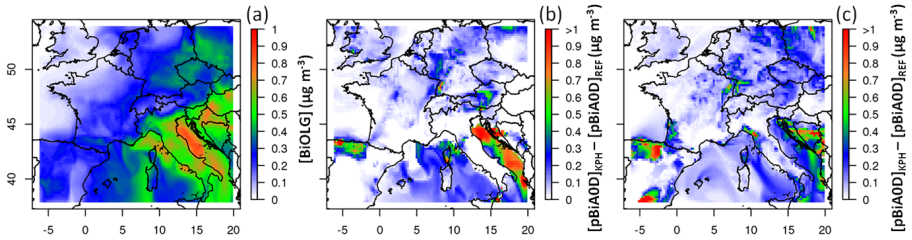

Figure 4. Oligomer daily maxima modeled with the two modeling approaches, using 3 different CHIMERE configurations for oligomer formation: KIN **(a)**, KPH Deliquescent **(b)** and KPH Metastable **(c)** for 24 July 2006.

GMDD
8, 9229–9279, 2015

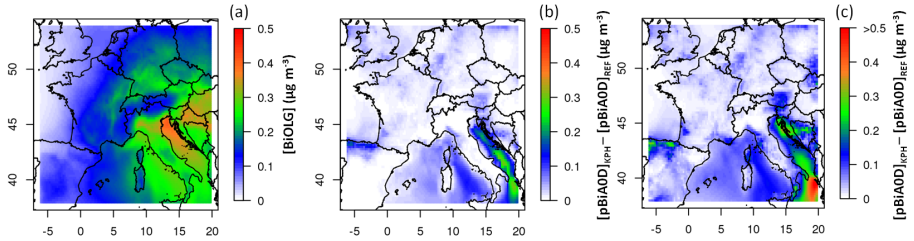

Figure 5. Average modeled oligomer concentration fields from monoterpenes in the KIN **(a)** and KPH configurations considering both deliquescent **(b)** and metastable mode **(c)** for the period of 20 July–3 August 2006.

GMDD
8, 9229–9279, 2015

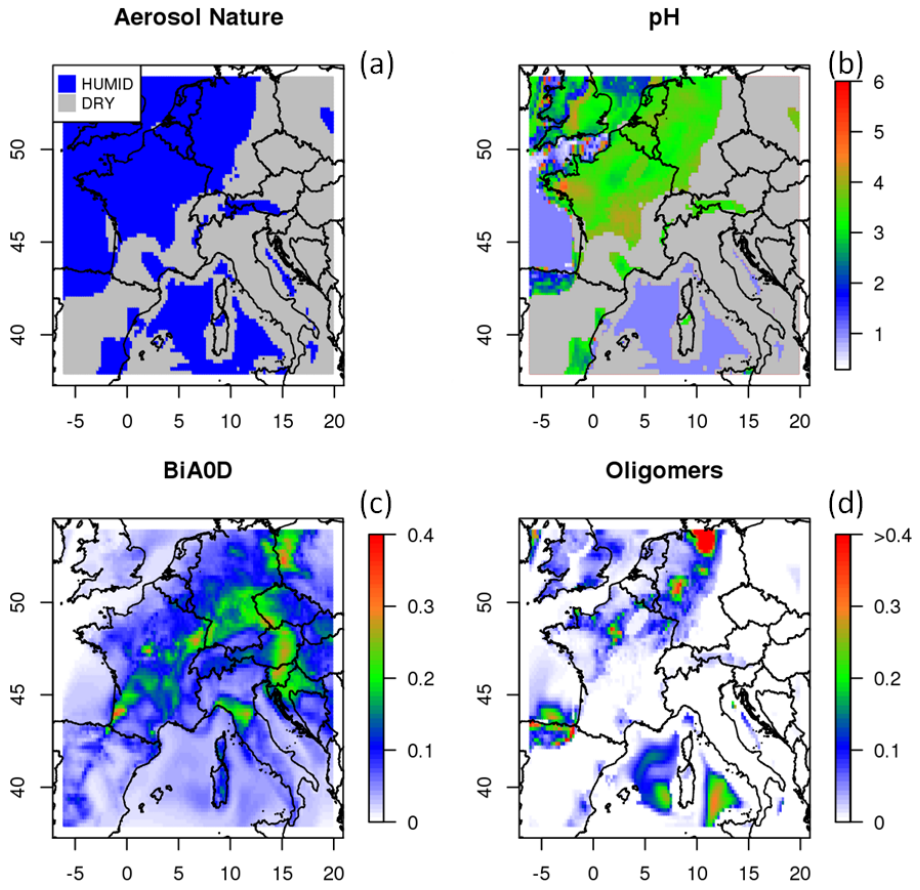

Figure 6. CHIMERE results for 24 July 2006 at 05:00 UTC: nature (humid or dry) of the aerosol **(a)**, pH of the aqueous phase **(b)**; BiA0D precursor concentration fields in the gas phase for the reference simulation ($\mu g\,m^{-3}$) **(c)** and oligomer concentrations ($\mu g\,m^{-3}$) **(d)** obtained with the KPH approach.

GMDD
8, 9229–9279, 2015

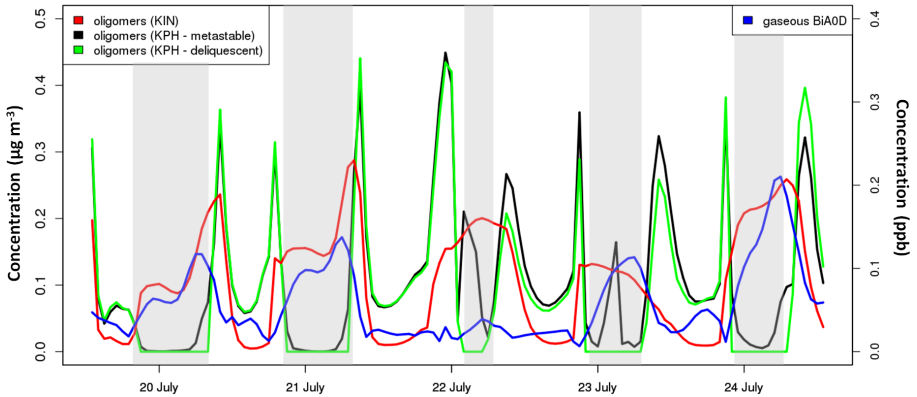

Figure 7. Time series of BiA0D concentrations (ppb) in the reference simulation (blue line), the KIN (red line) oligomer concentrations (µg m^{-3}), and the KPH oligomer concentrations (µg m^{-3}) in the deliquescent mode (green line) and in the metastable mode (black line), as simulated with CHIMERE for the 20–24 July 2006 period. The shaded areas correspond to the presence of a dry aerosol in the deliquescent configuration.

GMDD
8, 9229–9279, 2015

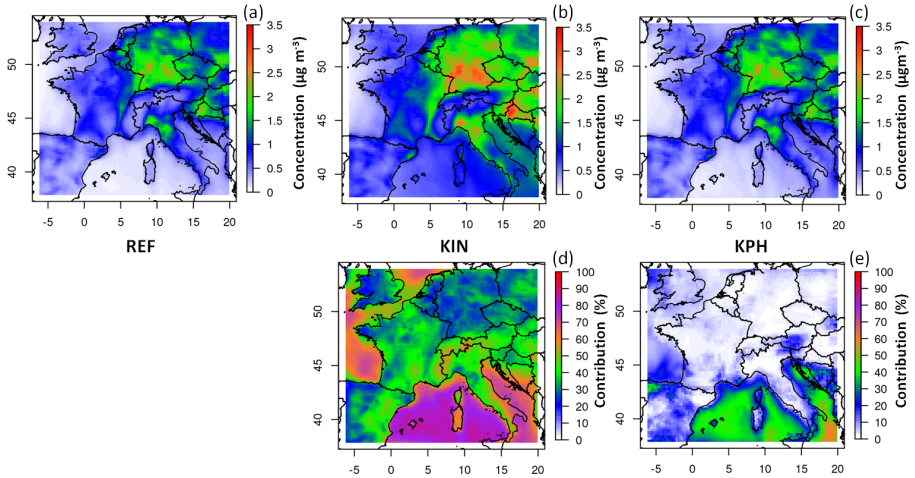

Figure 8. Modeled average BSOA concentration from monoterpenes simulated in the reference case (left), from the KIN approach (center) and from the KPH approach in the metastable mode (right) for the period 20 July–3 August 2006. Lower graph: contribution of oligomers to $BSOA_{terp}$.

GMDD
8, 9229–9279, 2015

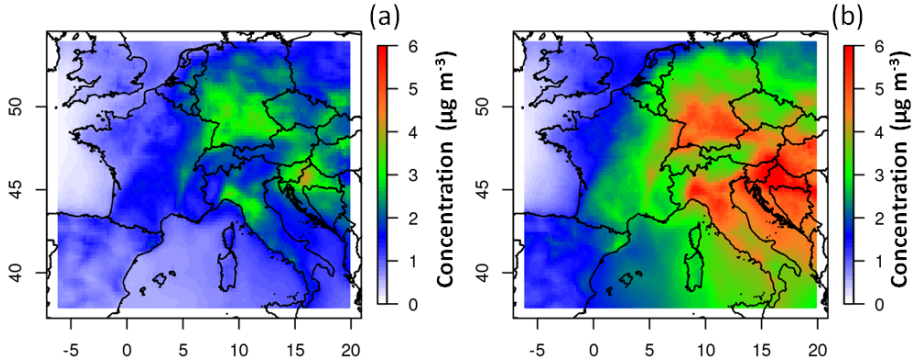

Figure 9. Modeled average BSOA concentration from isoprene and monoterpenes in the reference case (left) and from the KIN approach (right) for the period 20 July–3 August 2006.

GMDD
8, 9229–9279, 2015

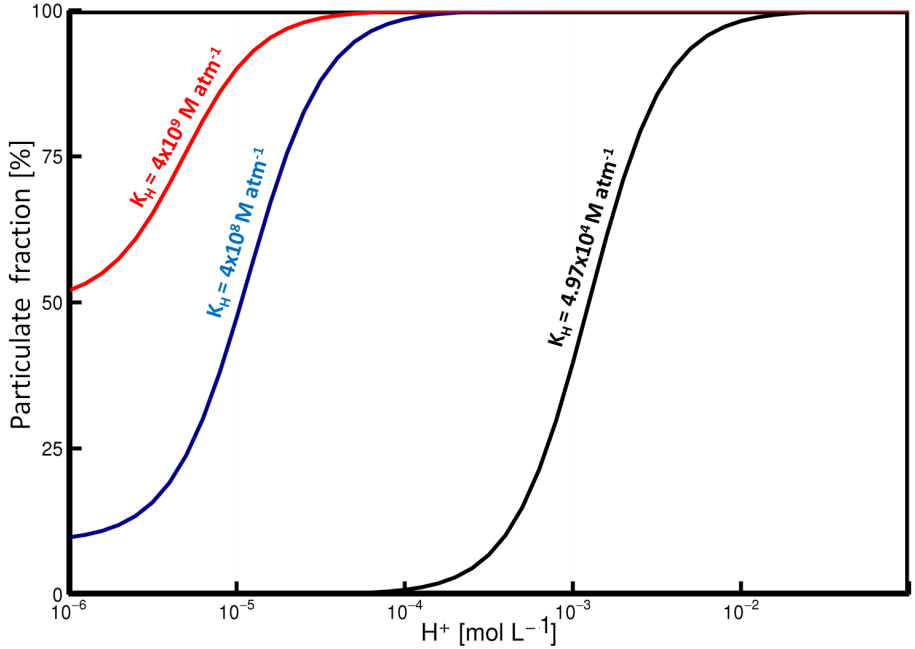

Figure 10. Evolution of the particulate fraction of a given species as a function of H^+ concentration, for 3 different values of its Henry's law constant $K_H = [4.97 \times 10^4; 4 \times 10^8; 4 \times 10^9\,\mathrm{M\,atm^{-1}}]$ at a LWC of $10^{-11}\,\mathrm{cm^3\,water\,cm^{-3}}$.

GMDD
8, 9229–9279, 2015

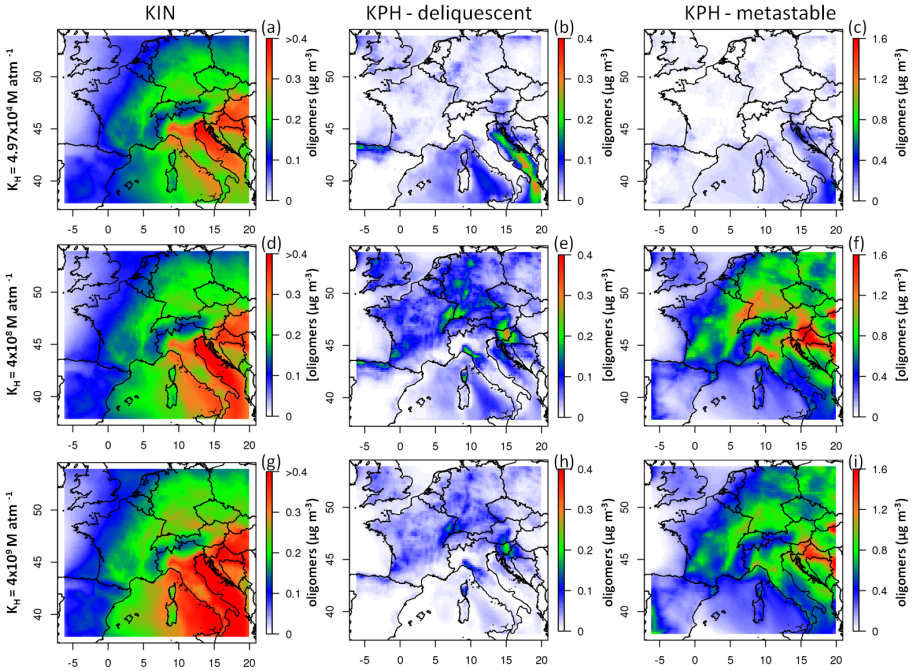

Figure 11. Mean modeled oligomer concentrations from monoterpenes hydrophilic surrogates (thus without BiBmP) for both approaches: KIN (left), KPH deliquescent (center) and KPH metastable mode (right) over 20 July–3 August 2006. The simulations are conducted using for BiA0D the following K_H values: 4.97×10^4 M atm^{-1} (top, **a**, **b** and **c**), 4×10^8 M atm^{-1} middle, (**d**, **e** and **f**) and 4×10^9 M atm^{-1} (bottom, **g**, **h** and **i**).

GMDD
8, 9229–9279, 2015